

1
2
3
4 Contrasting patterns of alteration at the Wheeler River area, Athabasca Basin,
5
6
7 Saskatchewan, Canada: Insights into the Zone K apparently uranium barren alteration
8
9 system.

10
11
12
13
14
15
16
17 **Jonathan Cloutier^{1*}, Kurt Kyser¹, Gema R. Olivo¹, Paul Alexandre¹**
18
19
20
21
22
23
24
25

26 ¹ Department of Geological Sciences and Geological Engineering Queen's University
27
28 Kingston, ON, Canada K7L 3N6
29
30
31
32
33
34
35
36
37
38
39
40
41
42
43
44
45
46
47
48
49
50
51
52
53
54
55
56
57
58
59
60
61
62
63
64
65

1
2
3
4 **Abstract**
5

6
7 Previous studies on Athabasca Basin unconformity-related uranium deposits have
8
9 focused on major deposits and have not investigated sites with barren alteration systems
10
11 that could clarify some of the critical factors controlling mineralization processes. A
12
13 paragenetic study of the Wheeler River area reveals the presence of minerals that formed
14
15 during the diagenetic, the main hydrothermal, which is subdivided into early, mid and
16
17 late hydrothermal substages, and the late alteration stages. The diagenetic stage consists
18
19 of early quartz overgrowths, siderite, rutile, hematite and abundant dickite in the pore
20
21 spaces of the Manitou Falls Formation. The early hydrothermal alteration substage is
22
23 characterized by pervasive 1Mc muscovite alteration and minor goyazite clusters, which
24
25 formed from oxidizing basinal fluids at temperatures around 240°C prior to 1550 Ma,
26
27 based on Ar-Ar dates. The mid hydrothermal alteration substage comprises dravite and
28
29 sudoite in the basal 200 meters of the Manitou Falls Formation, which are interpreted to
30
31 have formed at temperatures around 175°C from fluids chemically distinct but
32
33 isotopically similar to the basinal fluids involved during the early hydrothermal alteration
34
35 substage. The late hydrothermal substage was observed only at the Zone K of the
36
37 Wheeler River area and is characterized by the precipitation of clinocllore, copper
38
39 sulfides and florencite from reducing basement fluids emerging into the Manitou Falls
40
41 Formation at temperatures around 230°C, creating a ~250 meters high by ~250 meters
42
43 wide reducing halo. Oxidized uranium-bearing basinal fluids interacted with the Manitou
44
45 Falls Formation during the early hydrothermal substage prior to the arrival of the
46
47 reducing fluids during the mid and late hydrothermal substages and this precluded
48
49 uranium precipitation. The post hydrothermal alteration stage is characterized by
50
51
52
53
54
55
56
57
58
59
60
61
62
63
64
65

1
2
3
4 formation of kaolinite after late hydrothermal clinocllore near fractures by meteoric
5
6 waters. A minimal amount of leachable radiogenic Pb, with a Pb-Pb model age of 1907
7
8 Ma that is older age than both the Athabasca Basin and the main mineralization event of
9
10 1590 Ma, was encountered at the Zone K, indicating low probability of this area to host
11
12 uranium mineralization. However, areas of possible unconformity-related uranium
13
14 deposits were identified outside the Zone K wherein significant amounts leachable
15
16 radiogenic Pb were observed.
17
18
19
20
21

22 **Introduction**

23
24 Paleoproterozoic unconformity-type uranium deposits in the Athabasca Basin,
25
26 Canada, account for about one third of the global production of uranium (Krasenberg,
27
28 2004, Kyser and Cuney, 2008). These deposits are primarily hosted in the clastic
29
30 sediments of the Athabasca Group immediately above the unconformity or in the
31
32 underlying basement rocks, and are always surrounded by an extensive alteration halo
33
34 (e.g. Thomas et al., 1998; Jefferson et al., 2007; Kyser and Cuney, 2008). Typical
35
36 alteration associated with sandstone-hosted deposits consists predominantly of illite and
37
38 dickite with various amounts of chlorite, dravite, silicification and kaolinite (Kotzer and
39
40 Kyser, 1995, Thomas et al, 1998). The illite alteration generally defines an outer
41
42 alteration halo whereas overprinting of the illite alteration by chlorite and dravite defines
43
44 an inner halo. The mineralization in sandstone-hosted deposits is typically associated
45
46 with the chlorite-rich inner halo and is located at the intersection between high angle
47
48 reverse structures that cut the basement rocks and the basement-Athabasca Group
49
50 sediments unconformity. Alteration halos can be up to 400 meters wide at the base of the
51
52 Athabasca Group and may exceed several thousand meters in strike length (Thomas et
53
54
55
56
57
58
59
60
61
62
63
64
65

1
2
3
4 al., 1998; Jefferson et al., 2007; Kyser and Cuney, 2008). Trace elements observed with
5
6 sandstone-hosted mineralization are Ag, As, Au, Co, Cu, Ni, Mo, Pb, Pt group elements,
7
8 Se and Zn (Thomas et al., 1998; Jefferson et al., 2007; Kyser and Cuney, 2008).
9

10
11 Although most unconformity-related uranium deposits in the Athabasca Basin
12
13 have been extensively studied (e.g. Hoeve and Sibbald, 1978; Pagel et al., 1980; Sibald
14
15 and Quirt, 1987; Kotzer and Kyser, 1995; Fayek and Kyser, 1997), there remains
16
17 uncertainty about the critical factors needed to form these deposits and how to distinguish
18
19 them from similar alteration systems that lack economic mineralization. Most of the
20
21 previous studies focused on comparing the deposits (Pagel et al., 1980; Thomas et al.,
22
23 1998; Renac et al., 2002; Alexandre et al., 2005; Jefferson et al., 2007) and have not
24
25 investigated sites that lack economic mineralization. In this paper, we summarize the
26
27 results of a detailed petrological, geochemical and isotopic study of the Wheeler River
28
29 area. More precisely, the study focuses on the apparently barren Zone K alteration system
30
31 in the Wheeler River area, and on a transect located between the Zone K up to about 5km
32
33 from the McArthur River deposit. The section outside the Zone K was studied to verify if
34
35 any transition zones or anomalies were observed between the alteration zones present at
36
37 Zone K and the McArthur River U deposit. The alteration minerals, fluids, and
38
39 paragenetic relationships were used to develop a model for the genesis of the alteration
40
41 zones that is then compared with other models proposed for Athabasca Basin
42
43 unconformity-type uranium deposits.
44
45
46
47
48
49
50
51

52 **Regional Geology**

53
54
55 The Wheeler River area is situated in the Paleo- to Mesoproterozoic Athabasca
56
57 Basin, 25 km from the southeastern basin margin, 35 km southwest of the McArthur
58
59
60
61
62
63
64
65

1
2
3
4 River deposit and 25 km northeast of the Key Lake deposit (Fig. 1). The Athabasca Basin
5
6 is underlain by Archean and Paleoproterozoic rocks of the Hearne and Rae provinces
7
8 (Lewry and Sibbald, 1980; Hoffman, 1988; Tran et al., 2003; Fig. 1). On its eastern
9
10 margin, the basement of the Athabasca Basin is part of the Wollaston Domain. The
11
12 Wollaston Domain comprises four main groups of rocks (Lewry and Sibbald, 1980): (1)
13
14 the craton, a ca. 2.80-2.95 Ga Archean granitic, granodioritic, and tonalitic orthogneisses
15
16 and subordinate metamorphosed sedimentary rocks (Annesley et al., 2005); (2) a rift
17
18 sequence that host most of the mineralization, unconformable ~1.92 Ga high-grade
19
20 Paleoproterozoic pelitic (locally graphitic), psammopelitic, and psammitic gneisses,
21
22 subordinate metaquartzite, calc-silicates, and amphibolites, as well as rare BIF of the
23
24 Wollaston Group (Lewry and Sibbald, 1980; Tran et al., 2003); (3) a group that
25
26 unconformably overlies the upper part of sequence (2) and consists of a younger
27
28 sedimentary sequence related to continental collision with different lithologies and
29
30 geochemistry; (4) 1.80-1.84 Ga granitoids, gabbros and pegmatites (Annesley et al.,
31
32 2005). The rocks of the Wollaston Domain were complexly deformed and
33
34 metamorphosed to greenschist and amphibolite facies during the Trans-Hudson Orogen,
35
36 which reached peak metamorphism at ca. 1800–1820 Ma (Lewry and Sibbald, 1980;
37
38 Kyser et al., 2000).

39
40
41 The Athabasca Basin formed in response to rapid post-peak metamorphism uplift
42
43 of the Trans-Hudson Orogen at ca. 1750 Ma (Burwash et al., 1962; Kyser et al., 2000) as
44
45 a series of NE–SW oriented sub-basins, with the easternmost Cree sub-basin hosting the
46
47 majority of the known uranium deposits (Armstrong and Ramaekers, 1985). Sediments of
48
49 the Athabasca Basin consist of near-shore shallow shelf sequences of Paleoproterozoic to
50
51
52
53
54
55
56
57
58
59
60
61
62
63
64
65

1
2
3
4 Mesoproterozoic polycyclic, mature fluvial to marine quartz clastic sediments,
5
6 collectively referred to as the Athabasca Group (Ramaekers and Dunn, 1977; Ramaekers,
7
8 1990). In the eastern part of the Athabasca Basin, the Athabasca Group is comprised
9
10 exclusively of the Manitou Falls A, B, C and D members of unmetamorphosed clastic
11
12 sedimentary rocks (Fig. 2, 3b, c; Thomas, 2000). The basal portion of the Manitou Falls
13
14 Formation is composed of the Manitou Falls A and B members and consists of coarse-
15
16 grained conglomerate beds that reflect deposition in high energy braided streams, or
17
18 alluvial fan settings (e.g. Ramaekers, 1990). The upper portion of the Manitou Falls
19
20 Formation is composed primarily of the Manitou Falls B, C and D members and consists
21
22 of medium-grained sandstone with abundant ripple marks, rare thin mudstone layers, and
23
24 mud rip-up clasts with attributes that reflect deposition in lower energy distal braided
25
26 stream systems to possibly braid deltas (Ramaekers, 1990).
27
28
29
30
31
32

33
34 Ramaekers et al. (2007) proposed a revised stratigraphy of the Athabasca Group
35
36 introducing newly recognized Smart Formation in the western Athabasca and Read
37
38 Formation in the eastern Athabasca, which replace the A member of the Manitou Falls
39
40 Formation. They also subdivide the Manitou Falls Formation, introducing the Warnes
41
42 Member (MFw), Raibl Member (MFr) and Bird Member (MFb), that are the equivalent
43
44 of the Manitou Falls B member, but are attributed to the Karras deposystem for the
45
46 Warnes Member, the Moosonee deposystem for the Raibl Member, and the Ahenakew
47
48 deposystem for the Bird Member. To be consistent with past publications and industry
49
50 practices, this paper follows the original stratigraphy proposed by Ramaekers (1990) and
51
52 will refer to the Read Formation as the Manitou Falls A Member and the Warnes, Raibl
53
54 and Bird members of the Manitou Falls Formation as the Manitou Falls B Member.
55
56
57
58
59
60
61
62
63
64
65

1
2
3
4 Original detrital minerals in the Athabasca Group consisted of rounded quartz
5
6 with minor amounts of kaolinite, muscovite, montmorillonite, chlorite and heavy
7
8 minerals such as apatite, monazite, tourmaline and zircon (Hoeve and Quirt, 1984; Kotzer
9
10 and Kyser, 1995; Hiatt and Kyser, 2007). As sedimentation continued during the mid-
11
12 Proterozoic, the Athabasca Group reached a maximum thickness of 5-7 km (Pagel et al.,
13
14 1980) with temperatures near 200°C (Pagel et al., 1980; Hoeve and Quirt, 1984; Kotzer
15
16 and Kyser, 1995). This resulted in burial diagenesis of the Athabasca Group, converting
17
18 the detrital minerals to a mixture dominated by dickite, which defines the regional
19
20 background alteration, with lesser amounts of illite and chlorite (Quirt and Wasyliuk,
21
22 1997; Earle et al., 1999; Wasyliuk, 2002; Quirt, 2003). In the southeastern part of the
23
24 Athabasca Basin, Earle and Sopuck (1989) noted a large illite anomaly, which contains
25
26 subparallel linear zones of anomalous chlorite and dravite, overprinting the diagenetic
27
28 dickite regional pattern. The anomaly is associated with a 10–20 km wide corridor that
29
30 extends for 100 km and encompasses the Key Lake, McArthur River and the Millennium
31
32 deposits, but stops short of the Cigar Lake deposit (Fig. 2). Jefferson et al. (2007) noted
33
34 that the illite anomaly was overlying a 5–20 km wide aeromagnetic low, where
35
36 underlying Wollaston Supergroup gneiss includes abundant metaquartzite and metapelite
37
38 units, whereas the chlorite anomaly was spatially associated with quartzite ridges,
39
40 although it does not overlie all the known basement ridges. The anomaly was interpreted
41
42 by Wasyliuk (2002) to represent an area of increased fluid flux along or across large-
43
44 scale structural features.
45
46
47
48
49
50
51
52
53

54
55 The Athabasca Group and underlying basement are cut by a series of NW-SE
56
57 mafic dike swarms believed to be related to the Mackenzie dike swarms, with the most
58
59
60
61
62
63
64
65

1
2
3
4 prominent swarm dated at 1267 ± 2 Ma (U–Pb age in baddeleyite; LeCheminant and
5
6 Heaman 1989). They range from one to several hundred meters wide and are controlled
7
8 by tensional trends (Hoeve and Sibbald, 1978; Sibbald and Quirt, 1987). At present, the
9
10 total thickness of the sedimentary sequences is up to 2 km and the preserved detrital
11
12 minerals in the Athabasca Basin are composed of 95–100% well rounded quartz with
13
14 minor muscovite, kaolinite and rare heavy minerals, such as zircon and apatite (Kyser
15
16 and Cuney, 2008).
17
18
19
20
21
22
23

24 **Methodology**

25
26
27 A total of 115 representative drill core samples from the Manitou Falls Formation
28
29 and associated alteration were selected at different intervals from 16 drills holes during
30
31 the 2003 and 2004 sampling seasons. The samples taken during the first year are from
32
33 NNW-SSE and SSW-NNE transects along the Zone K (Fig. 3a, b, c). During the second
34
35 year of sampling, the SSW-NNE transect was extended to Read Lake, which is 5 km
36
37 away from the McArthur River unconformity-related uranium deposit. For each drill core
38
39 sampled, an effort was made to collect a sample from every member of the Manitou Falls
40
41 Formation and particular focus was given to altered zones. Typical samples vary in length
42
43 between 5 cm and 10 cm and have diameters of 2.5cm.
44
45
46
47

48
49 All samples were analyzed by Portable Infrared Mineral Analyzer (PIMA) to assist
50
51 with the identification of the clay minerals. The samples were then crushed and sieved
52
53 and clay-sized minerals were extracted from the coarsest fraction (>1.4 mm) by
54
55 ultrasound disintegration. Size separates were obtained using centrifugation, and X-ray
56
57 diffraction (XRD) analyses were performed on all size fractions (i.e. <2 μm , 2-5 μm and
58
59
60
61
62
63
64
65

1
2
3
4 >5 μm) using a Siemens X-Pert installation at Queen's University, Kingston, Canada.
5
6

7 Quantitative analyses of the alteration minerals were determined on an automated
8
9 4-spectrometer Cameca Camebax MBX electron probe by the wavelength dispersive X-
10 ray analysis method (WDS) at Carleton University in Ottawa. Operating conditions were:
11 15kv accelerating voltage, 20 nano-amperes (nA) beam current for oxides and silicates.
12
13 Specimens were analyzed using a rastered electron beam 5x5 to 10x10 microns in size.
14
15 Counting times were 15-40 seconds or 40,000 accumulated counts. Background
16
17 measurements were made at 50% peak counting time on each side of the analyzed peak.
18
19 Background positions were carefully selected to avoid instances of peak overlap. Raw X-
20
21 ray data were converted to elemental weight % by the Cameca PAP matrix correction
22
23 program. A suite of well characterized natural and synthetic minerals and compounds
24
25 were used as calibration standards. Analyses are accurate to 1-2 % relative for major
26
27 elements (>10 wt %), 3-5 % relative for minor elements (>0.5 - <5.0 wt %). The
28
29 chemical compositions of chlorite and muscovite were used to estimate temperatures of
30
31 formation based on tetrahedral site occupancy of Cathelineau (1988) and are accurate to
32
33 within 30°C.
34
35
36
37
38
39
40
41
42

43 Stable oxygen isotopic compositions were measured using a dual inlet Finnigan
44
45 MAT 252 isotopic ratio mass spectrometer. Oxygen was extracted using the BrF_5 method
46
47 of Clayton and Mayeda (1963). Hydrogen isotopic compositions were determined using a
48
49 TC/EA ThermoFinnigan and a DeltaPlus XP Finnigan MAT mass spectrometer. Oxygen
50
51 and hydrogen isotopic ratios are reported in the δ notation in units of per mil relative to
52
53 Vienna Standard Mean Ocean Water (V-SMOW) standard. $\delta^{18}\text{O}$ and δD analyses were
54
55 reproducible to ± 0.2 and ± 3 per mil, respectively. Oxygen isotope fractionation factors
56
57
58
59
60
61
62
63
64
65

1
2
3
4 used throughout this paper are those proposed by Wenner and Taylor (1971) for water-
5
6 chlorite, O'Neil and Taylor (1969) for water-muscovite and water-kaolinite. Hydrogen
7
8 isotope fractionation factors used are those proposed by Marumo et al. (1980) for water-
9
10 chlorite, Vennemann and O'Neil (1996) for water-muscovite and Sheppard and Gilg
11
12 (1996) for water-kaolinite. In previous studies, the water-illite fractionation factor of Yeh
13
14 (1980) was used instead of the one of Vennemann and O'Neil (1996) for water-
15
16 muscovite. Hydrogen water-illite fractionation factors of Yeh (1980) used in previous
17
18 studies were calibrated in the Texas Gulf Coast and used a natural diagenesis progression
19
20 from kaolinite to smectite to illite/smectite to illite for hydrogen. The illite chemical
21
22 composition from the Texas Gulf Coast varies between 2-6% K₂O and 2- 6% FeO
23
24 (Awwiller, 1993) and is different from the chemical composition of the white mica
25
26 present in the alteration zones of the Athabasca Basin, where K₂O generally varies
27
28 between 8 and 10% and FeO is usually <1% (Wilson and Kyser, 1987; Kotzer and Kyser,
29
30 1995; Alexandre et al. 2005). Moreover, Vennemann and O'Neil (1996) pointed out that
31
32 Fe content has the strongest effect on the fractionation of hydrogen-mineral, wherein the
33
34 water-mineral fractionation factor increases with decreasing Fe content. Therefore we
35
36 prefer the muscovite-water fractionation factor of Vennemann and O'Neil (1996). The
37
38 δD values of the fluids are 38‰ higher at 250°C using the muscovite-water fractionation
39
40 factors relative to those using illite-water.
41
42
43
44
45
46
47
48
49

50 ⁴⁰Ar/³⁹Ar dating was done on five pure monomineralic separates of muscovite and
51
52 one of chlorite (2 to 5 μm size fraction). The Ar present in chlorite is from muscovite
53
54 impurities within the chlorite sheets. Clay and silt size mineral dating using ⁴⁰Ar/³⁹Ar is
55
56 often difficult to interpret as clay size minerals have relatively low argon retention
57
58
59
60
61
62
63
64
65

1
2
3
4 (McDougall and Harrison, 1999), which make them more susceptible to partial
5
6 radiogenic argon loss and $^{39}\text{Ar}_K$ recoil resulting in few plateau ages. The $^{40}\text{Ar}/^{39}\text{Ar}$ dating
7
8 was done at the Scottish Universities Environmental Research Centre in Glasgow
9
10 (SUERC), United Kingdom and at the Noble Gas Laboratory, Pacific Centre for Isotopic
11
12 and Geochemical Research, University of British Columbia. Plateau ages were calculated
13
14 using not less of 70% of the gas released and three consecutive steps that overlap in their
15
16 1σ error margin while pseudo-plateau ages were defined by 30-70 % of the gas released.
17
18 The samples were irradiated at the McMaster Nuclear Reactor in Hamilton, Ontario, for
19
20 90 MWH, with a neutron flux of approximately 6×10^{13} neutrons/cm²/s. All measurements
21
22 were corrected for total system blank, mass spectrometer sensitivity, mass discrimination,
23
24 radioactive decay during and subsequent to irradiation, as well as interfering Ar from
25
26 atmospheric contamination and the irradiation of Ca, Cl and K.
27
28
29
30
31
32

33
34 One hundred and eleven Manitou Falls Formation samples were analyzed for
35
36 leachable trace elements and for Pb and U isotopes following the technique of Holk et al.
37
38 (2003). Forty five samples were from the Zone K, sixty five were from outside the Zone
39
40 K and one was from a mineralized basement sample from the Read Lake area that
41
42 contains a 0.3 mm wide uraninite veins. The 0.50–1.40 mm crushed fraction was used
43
44 and about 0.5 g of sample and 5 ml of 0.02 M HNO₃ spiked with ^{115}In were loaded into a
45
46 polyurethane tube, placed in an ultrasonic bath for 120 min and centrifuged. One gram of
47
48 the liquid was diluted with 100 g of the spiked acid reagent and the Pb isotopic ratios and
49
50 trace element concentrations were measured using a Finnigan MAT ELEMENT HR-ICP-
51
52 MS. The Pb and U isotope ratios were calculated using the signal intensities (counts/s) in
53
54 low-resolution mode and have an uncertainty of ca. 1% based on repeat analyses.
55
56
57
58
59
60
61
62
63
64
65

1
2
3
4 Corrections were made for interferences from Hg and mass fractionation was monitored
5
6 using Tl in the solutions and externally with in-house and NIST Pb isotope standards
7
8 (NBS 981 and NBS 983). For each sample, ^{201}Hg , ^{202}Hg , ^{204}Pb , ^{206}Pb , ^{207}Pb , ^{208}Pb , ^{235}U
9
10 and ^{238}U were measured, blank subtracted and ^{204}Pb was corrected for ^{204}Hg interference
11
12 using ^{202}Hg . Concentrations were corrected for instrument drift and matrix using ^{115}In as
13
14 an internal standard and external calibration for element concentrations and blank
15
16 subtraction. $^{206}\text{Pb}/^{204}\text{Pb}$ ratios greater than 30 are considered radiogenic in order to
17
18 differentiate between today $^{206}\text{Pb}/^{204}\text{Pb}$ normal ratio of 17 and true radiogenic samples.
19
20
21
22
23
24
25

26 **Local Geology**

27
28 The Athabasca Group sedimentary rocks in the Wheeler River area range in
29
30 thickness from 100 to 600 m and are comprised exclusively of Manitou Falls D, C, B and
31
32 A members of unmetamorphosed clastic sedimentary rocks (Fig. 3b, c; Thomas, 2000).
33
34 The Wheeler River area is located within the regional illite anomaly noted by Earle and
35
36 Sopuck (1989) and the alteration associated with the Manitou Falls Formation throughout
37
38 the Wheeler River area consists of a mixture dominated by illite and lesser dickite (Fig. 2,
39
40 3b, c; Earle and Sopuck, 1989; Thomas, 2000, Wasyluk, 2002). A pale green chlorite
41
42 alteration is also observed within the Manitou Falls A, B, C members but mainly near the
43
44 unconformity at Zone K and in drill hole WR188 within the Manitou Falls A, C and D
45
46 members outside the Zone K (Fig. 3b, c).
47
48
49
50
51

52
53 At Zone K, the regional illite-dickite alteration is overprinted by a dark green
54
55 chloritic alteration halo within the Manitou Falls A and B members in the proximity of a
56
57 reverse fault originating from the basement rocks (Fig. 3b, c; Thomas, 2000). This green
58
59
60
61
62
63
64
65

1
2
3
4 chlorite halo is associated with a Cu, Fe, Ni and S enrichment as pyrite and copper
5
6 sulfides, indicating reducing conditions at the time of formation, and a weak U
7
8 enrichment up to 4 ppm (S. McHardy, pers. comm., 1997), compared to 1ppm in the
9
10 surrounding sedimentary rocks. Strong kaolinite alteration was also observed in the
11
12 Manitou Falls C and D members in Zone K drill holes ZK17, ZK22, WR192 and ZQ15,
13
14 whereas a dravite-dominant alteration was noted in drill hole 84-7 and close to the
15
16 surface in drill hole WR192 (Fig. 3b, c). Their mineral chemistry and textural
17
18 relationships are described in detail in the following sections.
19
20
21
22
23
24
25

26 **Mineral Paragenesis**

27
28 Three main stages of alteration were identified in the Manitou Falls Formation in
29
30 the Wheeler River area: diagenesis, hydrothermal alteration (subdivided into early, mid
31
32 and late substages), and post-hydrothermal alteration (Fig. 4). The diagenesis stage was
33
34 defined as regional background alteration associated with the burial of the Manitou Falls
35
36 Formation that affected the majority of the Athabasca Basin, whereas the hydrothermal
37
38 stage was defined as local alteration events associated with, or in close proximity to,
39
40 uranium deposits in previous studies (Wilson and Kyser, 1987; Kotzer and Kyser, 1995;
41
42 Thomas et al., 1998; Jefferson et al., 2007; Kyser and Cuney, 2008. Detrital minerals
43
44 preserved in the Manitou Falls Formation prior to diagenesis are, by order of importance,
45
46 quartz, muscovite, ilmenite, zircon, apatite and tourmaline (Fig. 4).
47
48
49
50
51
52

53 The earliest diagenetic features preserved are red-brown H1 hematite stains around
54
55 detrital quartz grains and subsequent poorly- to well-preserved syn-compaction Q1 quartz
56
57 overgrowths (Fig. 5a). Minor Sd1 siderite (50-500 μ m) is observed in the pore space of
58
59
60
61
62
63
64
65

1
2
3
4 the Manitou Falls C and D members throughout the studied area. Recrystallization of
5
6 detrital ilmenite and Fe-oxides to fine-grained H2 hematite and R1 rutile needles
7
8 occurred subsequent to Q1 quartz precipitation. Precise timing between Sd1 siderite and
9
10 R1 rutile and H2 hematite cannot be determined as Sd1 siderite was not observed in close
11
12 proximity to R1 rutile and H2 hematite. A late diagenetic feature consists of precipitation
13
14 of medium- to fine-grained euhedral K1 dickite (<200µm) in the pore space of the
15
16 Manitou Falls Formation throughout the study area, which fills the embayments of Q1
17
18 quartz, Sd1 siderite, R1 rutile and H2 hematite (Fig. 5b).
19
20
21
22

23
24 The early hydrothermal alteration substage consists of weak to pervasive
25
26 replacement of detrital K0 kaolinite and diagenetic K1 dickite by fine-grained Ms1
27
28 muscovite (<200µm) along intergrain contacts and interlayer sheets (Fig. 5b,c). Minor
29
30 amounts of very fine-grained euhedral aluminum phosphate-sulfate mineral (APS1)
31
32 clusters (1-5µm) are observed throughout the study area, and are present in pore spaces
33
34 between the muscovite crystals or sheet layers and are interpreted to be coeval or slightly
35
36 older than Ms1 muscovite. K1 dickite and Ms1 muscovite minerals are similar to those
37
38 observed to be pre-mineralization in some other sandstone-hosted uranium deposits such
39
40 as McArthur River, Key Lake and Cigar Lake (Kotzer et al., 1995; Fayek et al., 1997;
41
42 Cuney and Kyser, 2008).
43
44
45
46
47

48 The mid hydrothermal alteration substage is characterized by the occurrence of T1
49
50 dravite as aggregates of fine- to medium-grained acicular crystals (50-500µm) growing
51
52 from the edge of Q0 and Q1 quartz (Fig. 5d) and veinlets with minor coeval Q2 quartz
53
54 crosscutting K1 dickite and Ms1 muscovite. This T1 dravite alteration is followed by
55
56 pervasive alteration of K1 dickite, Ms1 muscovite and T1 dravite to fine-grained pale
57
58
59
60
61
62
63
64
65

1
2
3
4 green C1 chlorite (<50µm) mainly in the Manitou Falls A member. C1 chlorite fills
5
6 embayments of K1 dickite and Ms1 muscovite and corroded zones of T1 dravite (Fig.
7
8 5d). T1 dravite and C1 chlorite are similar to those observed to be post mineralization in
9
10 other sandstone-hosted uranium deposits such as McArthur River, Key Lake and Cigar
11
12 Lake (Kotzer et al., 1995; Fayek et al., 1997; Cuney and Kyser, 2008).
13
14

15
16 The late hydrothermal stage is characterized by a pervasive alteration of previous
17
18 diagenetic and hydrothermal alteration stage minerals to fine-grained dark green C2
19
20 chlorite (<50µm) delineating a ~250 meters high with a ~250 meters diameter alteration
21
22 zone (Fig. 3b,c). C2 chlorite occurs at Zone K in drill hole ZK12, ZK13, ZK 17and ZK22
23
24 and outside the Zone K near the unconformity in drill hole WR192 (Fig. 3b, c). C2
25
26 chlorite fills embayments of K1 kaolinite and Ms1 muscovite, and veinlets of C2 chlorite
27
28 crosscut C1 chlorite alteration (Fig. 5e). C2 chlorite is coeval with pyrite, chalcopyrite
29
30 and APS minerals (APS2).
31
32
33
34

35
36 The post hydrothermal alteration stage is the last event recorded and consists of
37
38 minor fine-grained K2 kaolinite (<50µm) pseudomorphously replacing C2 chlorite near
39
40 fracture zones (Fig. 5f).
41
42
43
44

45 **Mineral Chemistry of the Alteration Phases**

46
47 Early hydrothermal substage muscovite at Zone K (a subset of Ms1 muscovite
48
49 termed Ms1_k) has an average chemical composition of 48.1% SiO₂, 33.2% Al₂O₃, 9.3%
50
51 K₂O, 1.2% FeO and 1.0% MgO. The calculated average structural formula is
52
53 $K_{0.79}Mg_{0.10}Fe_{0.07}Al_{1.83}(Si_{3.23},Al_{0.77})O_{10}(OH)_2$ with K varying from 0.62 to 0.89 atoms per
54
55 formula unit (apfu), indicating a formation temperature of 240°C (Table 1; Cathelineau,
56
57
58
59
60
61
62
63
64
65

1
2
3
4 1988). Muscovites outside Zone K (a subset of Ms1 muscovite termed Ms1_o) have an
5
6 average chemical composition of 47.8% SiO₂, 33.7% Al₂O₃, 9.5% K₂O, 0.7% FeO and
7
8 0.7% MgO. The calculated average structural formula is
9
10 $K_{0.82}Mg_{0.07}Fe_{0.04}Al_{1.90}(Si_{3.22},Al_{0.78})O_{10}(OH)_2$, with K varying from 0.74 to 0.87 apfu, also
11
12 indicating a formation temperature near 240°C (Table 1; Cathelineau, 1988). Muscovite
13
14 at Zone K (Ms1_k) has slightly higher Fe and Mg contents and more variable K content
15
16 than Ms1_o muscovite outside Zone K (Table 1). Although, Ms1_k muscovites show a
17
18 greater chemical variation than Ms1_o muscovites (Fig. 6a), both Ms1_k and Ms1_o
19
20 muscovites are closer to the theoretical composition of muscovite than to that of illite on
21
22 a SiO₂, K₂O and Al₂O₃ ternary diagram (Fig. 6b). Their compositions are also similar to
23
24 the Athabasca Basin white mica termed “illite” in previous publications (e.g. Hoeve and
25
26 Sibbald, 1978; Kotzer and Kyser, 1995; Fayek and Kyser, 1997). Therefore, the term
27
28 muscovite used in this paper will refer to the same white mica called illite in previous
29
30 publications.
31
32
33
34
35
36
37

38 The average chemical composition of APS1 minerals is 9.87% SrO, 2.52% CaO,
39
40 1.94% La₂O₃, 4.41% Ce₂O₃, 1.24% Nd₂O₃, 4.77% SO₃, 20.81% P₂O₅, 3.21% FeO and
41
42 31.07% Al₂O₃ with minor amounts of F, BaO and ThO₂ (Table 2). The calculated
43
44 structural formulas is $Sr_{0.45}Ca_{0.21}LREE_{0.24}Th_{0.03}(Al_{2.88}Fe_{0.21})(PO_4)_{1.39}(SO_4)_{0.28}(OH)_6$,
45
46 corresponding to goyazite. The average chemical composition of APS2 minerals is 4.12%
47
48 SrO, 1.81% CaO, 4.43% La₂O₃, 9.37% Ce₂O₃, 3.02% Nd₂O₃, 2.59% SO₃, 20.96% P₂O₅,
49
50 2.46% FeO and 28.93% Al₂O₃ with minor amounts of F, BaO and ThO₂ (Table 2). The
51
52 calculated average structural formula is
53
54
55
56
57 $Sr_{0.21}Ca_{0.17}LREE_{0.55}Th_{0.01}(Al_{2.95}Fe_{0.17})(PO_4)_{1.53}(SO_4)_{0.17}(OH)_6$, corresponding to
58
59
60
61
62
63
64
65

1
2
3
4 florencite. APS2 mineral chemistry differs from that of APS1 by having less SrO and
5
6 greater LREE elements (Fig. 7).
7

8
9 C1 chlorites at Zone K (a subset of C1 chlorite termed C1_k) are Mg-Al-rich
10 chlorite with an average chemical composition of 33.5% SiO₂, 28.2% Al₂O₃, 10.2% MgO
11 and 1.4% FeO. The calculated average structural formula is
12
13
14
15
16 $Mg_{3.12}Fe_{0.23}Al_{5.95}(Si_{7.01},Al_{0.99})O_{20}(OH)_{16}$ (Table 1), corresponding to sudoite and a
17
18 formation temperature near 175°C. In contrast, C2 chlorites are Mg-Fe-rich chlorites with
19 an average chemical composition of 29.8% SiO₂, 21.8% MgO, 19.2% Al₂O₃ and 7.4%
20 FeO and are chemically different than C1 chlorite. The calculated average structural
21
22
23
24
25
26
27
28
29
30
31
32
33
34
35
36
37
38
39
40
41
42
43
44
45
46
47
48
49
50
51
52
53
54
55
56
57
58
59
60
61
62
63
64
65

formula is $Mg_{6.89}Fe_{1.31}Al_{3.07}(Si_{6.30},Al_{1.70})O_{20}(OH)_{16}$ (Table 1), corresponding to
clinochlore and a formation temperature near 230°C. The chemical compositions of C1
and C2 chlorites vary from Al-rich to Mg-Fe-rich end-members, suggesting that the final
chemical composition of the chlorites resulted from alteration of C1 sudoite by a Mg-rich
fluid, which precipitated C2 clinochlore, and eventually replaced C1 sudoite with C2
clinochlore (Fig. 8). The original composition of C1 sudoite would therefore be related to
the chlorites which plot closer to the Al pole while the true composition of C2 clinochlore
would be associated with the chlorites which plot closer to the Mg pole on the Al-Mg-Fe
ternary diagram (Fig. 8).

X-Ray Diffraction of Ms1 Muscovite

XRD data from seven separates of Ms1_k muscovite and eight separates of Ms1_o
muscovite indicate the presence of 2 polytypes within the Wheeler River area (Fig. 9a,b,
10). Ms1_k muscovites from Zone K show a mixture between the 1Mc polytype and the

1
2
3
4 1Mt polytype (Fig. 9a), whereas Ms1_o muscovites from outside Zone K are dominated by
5
6 the 1Mc polytype (Fig. 9b). Samples close to the unconformity from both zones record an
7
8 increasing amount of the 1Mt muscovite polytype. 1Mc muscovites are associated with
9
10 rigid, micrometer-scale lath-shaped Ms1 muscovite crystals (Fig. 10a, b, c, d), whereas
11
12 1Mt muscovites are associated with thin, sub-micrometer, “hairy”-shaped Ms2 muscovite
13
14 crystals growing on the edge of Ms1 (1Mc) muscovites (Fig. 10a, b, c, d).
15
16
17
18
19
20

21 **Isotopic Composition of Alteration**

22
23 Stable isotopic compositions were determined for early hydrothermal alteration
24
25 substage Ms1_k and Ms1_o muscovites, mid hydrothermal alteration substage C1_k and C1_o
26
27 sudoite, late hydrothermal alteration substage C2 clinocllore, and post hydrothermal
28
29 alteration stage K2 kaolinite (Table 3, Fig. 11).
30
31

32 *Early hydrothermal alteration substage muscovite (Ms1)*

33
34 Measured $\delta^{18}\text{O}$ and δD values of twelve Ms1_k muscovites from Zone K vary from
35
36 +7.3 to +12.0 per mil for $\delta^{18}\text{O}$ and -62 to -37 per mil for δD (Table 3). Using the
37
38 formation temperature of 240°C for Ms1_k muscovite obtained from mineral chemistry
39
40 (Table 1), the calculated $\delta^{18}\text{O}$ values of the fluid in equilibrium with Ms1_k muscovite
41
42 range from +2.1 to +6.8 per mil, and δD values range from -32 to -7 per mil (Fig. 11;
43
44 Table 3). Measured $\delta^{18}\text{O}$ and δD values of nine Ms1_o muscovites outside Zone K vary
45
46 from +10.1 to +12.0 per mil for $\delta^{18}\text{O}$ and -66 to -52 per mil for δD (Table 3). Using
47
48 formation temperatures of 240°C for Ms1_o muscovite obtained from mineral chemistry
49
50 (Table 1), the calculated $\delta^{18}\text{O}$ values of the fluid in equilibrium with Ms1_o muscovites,
51
52 which are outside Zone K, range from +4.9 to +6.8 per mil, and the δD values range from
53
54
55
56
57
58
59
60
61
62
63
64
65

1
2
3
4 -36 to -22 per mil (Fig. 11; Table 3). Muscovites from Zone K are more variable, with
5
6 higher δD_{H_2O} and lower $\delta^{18}O_{H_2O}$ values than those from outside Zone K (Fig.11).
7
8

9
10 *Mid hydrothermal alteration substage sudoite (C1)*
11

12
13 Measured $\delta^{18}O$ and δD values of one separate of $C1_k$ sudoite from Zone K and one
14
15 separate of $C1_o$ sudoite from outside Zone K have values of +10.4 and +9.3 per mil for
16
17 $\delta^{18}O$ and -59 and -62 per mil for δD , respectively. Using a formation temperature of
18
19 175°C obtained on $C1_k$ sudoites (Table 1), the calculated values for the fluid in
20
21 equilibrium with $C1_k$ sudoites are +7.3 per mil for $\delta^{18}O$ and -27 per mil for δD , and +6.2
22
23 per mil for $\delta^{18}O$ and -30 per mil for δD for $C1_o$ (Fig. 11; Table 3). The formation
24
25 temperature of 175°C can be used as a good approximation of the real formation
26
27 temperature for $C1_o$ sudoite as it is paragenetically related to $C1_k$ sudoite, and a similar
28
29 formation temperature of 180°C was concluded by Kotzer and Kyser (1995) for sudoites
30
31 all over the eastern Athabasca Basin. The $\delta^{18}O$ and δD values obtained on C1 sudoites are
32
33 similar to those obtained on Ms1 muscovites.
34
35
36
37
38
39
40

41 *Late hydrothermal alteration substage clinochlore (C2)*
42

43
44 Measured $\delta^{18}O$ and δD values of eight C2 clinochlores are between +2.8 and +6.3
45
46 per mil and -64 and -37 per mil, respectively. Using a formation temperature of 230°C for
47
48 C2 chlorites obtained from mineral chemistry (Table 1), the calculated $\delta^{18}O$ values for
49
50 the fluid in equilibrium with C2 clinochlores are between +1.4 and +4.8 per mil and -37
51
52 and -10 per mil for δD (Fig. 11; Table 3). C2 clinochlores have lower $\delta^{18}O$ values than
53
54 Ms1 muscovites and C1 sudoites but similar δD values.
55
56
57
58

59 *Post hydrothermal alteration kaolinite (K2)*
60
61
62
63
64
65

1
2
3
4 Measured $\delta^{18}\text{O}$ and δD values of six K2 kaolinites are between +6.6 and +11.9 per
5
6 mil for $\delta^{18}\text{O}$ and between -120 and -88 per mil for δD (Table 3). The isotopic
7
8 compositions of K2 kaolinites are similar to kaolinite that forms from meteoric waters at
9
10 around 50°C. The calculated $\delta^{18}\text{O}$ and the δD values for the fluid in equilibrium with K2
11
12 kaolinites at a temperature of 50°C are between -13.1 and -7.8 per mil and -92 and -59
13
14 per mil respectively (Fig. 11; Table 3).
15
16
17
18

19 $^{40}\text{Ar}/^{39}\text{Ar}$ Geochronology

20
21
22 $^{40}\text{Ar}/^{39}\text{Ar}$ dating of three Ms1_k muscovites and two 1sM_o muscovites have pseudo-
23
24 plateau dates of 1216 ± 6 Ma, 1237 ± 7 Ma and 1497 ± 20 Ma and 1298 ± 7 Ma and 1356
25
26 ± 7 Ma, respectively (Fig. 12a-e; Table 4). The gas released for the pseudo plateaus for
27
28 muscovite from both zones varies between 35.6 and 67.4%. C1_k Mg-Al-rich chlorite has
29
30 a plateau $^{40}\text{Ar}/^{39}\text{Ar}$ date of 1548 ± 23 Ma, corresponding to 75.2% of the total gas
31
32 released (Fig. 12f) and is interpreted to represent the maximum age at which C1_k sudoite
33
34 replaced Ms1 muscovite during the mid hydrothermal event.
35
36
37
38

39 The 1497 Ma (Ms1_k) and 1548 Ma (C1_k) dates are younger than the 1590 Ma main
40
41 mineralization event for both basin- and basement-hosted deposits throughout the
42
43 Athabasca Basin (Alexandre et al., 2009). However, they are similar to those of the
44
45 $^{40}\text{Ar}/^{39}\text{Ar}$ perturbation stage at ca. 1525 Ma attributed to fluid movement associated with
46
47 the distal Mazatzal Orogeny (Alexandre et al., 2009). Two other perturbations of the
48
49 $^{40}\text{Ar}/^{39}\text{Ar}$ systematics are recorded in muscovite and chlorite grains at ca. 1350 and 1215-
50
51 1300. These resetting events are common in sandstone-hosted deposits and correspond to
52
53 fluid circulation in the Athabasca Basin induced by far-field tectonic events (Alexandre et
54
55 al, 2009). The 1356 ± 7 Ma $^{40}\text{Ar}/^{39}\text{Ar}$ date is interpreted to reflect a fluid resetting event
56
57
58
59
60
61
62
63
64
65

1
2
3
4 in the Ar system during the Berthoud Orogeny in southwest USA (Nyman et al., 1994;
5
6 Sims and Stein, 2001) whereas the 1215-1300 Ma dates correspond to the emplacement
7
8 of the MacKenzie dike swarms across the Athabasca Basin (LeCheminant and Heaman,
9
10 1989). Although these later events affected the Ar-Ar systematics, the H and O isotopic
11
12 compositions were not affected because the latter do not vary with Ar age.
13
14
15
16
17
18

19 **Chemistry and Geochronology of the Weak Acid**

20
21 Leachable Pb present in a sample can be uranium supported or unsupported based
22
23 on the $^{206}\text{Pb}/^{204}\text{Pb}$ and $^{238}\text{U}/^{206}\text{Pb}$ ratios (Holk et al. 2003). The leachable Pb present is
24
25 said to be supported when its presence can be attributed to the amount of leachable
26
27 uranium present in the sample. The uranium-supported Pb can be often attributed to local
28
29 uraninite grains as well as detrital minerals containing uranium such as apatite, monazite
30
31 and zircon. The leachable Pb is said to be unsupported when it cannot be attributed to the
32
33 amount of leachable uranium present in the sample and the time since the deposits
34
35 formed at 1590 Ma (Alexandre et al., 2009).
36
37
38
39
40

41 Pb isotopic compositions of leachates reveal the presence of radiogenic Pb
42
43 ($^{206}\text{Pb}/^{204}\text{Pb} > 30$) (Appendix I) in Zone K (Fig. 13), although the range is between 17-
44
45 105 and averages 34. High $^{206}\text{Pb}/^{204}\text{Pb}$ ratios are observed near the unconformity (Fig.
46
47 13). A $^{207}\text{Pb}/^{206}\text{Pb}$ model age of uranium-unsupported radiogenic Pb at Zone K is $1907 \pm$
48
49 140 Ma (Fig. 14), older than the 1590 Ma main mineralization event in the Athabasca
50
51 Basin (Alexandre et al., 2009). Pb leached from the Manitou Falls Formation outside
52
53 Zone K is radiogenic with $^{206}\text{Pb}/^{204}\text{Pb}$ ratios greater than 19, most having ^{204}Pb below
54
55 detection limit.
56
57
58
59
60
61
62
63
64
65

1
2
3
4 Leachable elements that correlate with uranium in uranium-supported samples
5
6 from Zone K include Ca, P, Pb and Sr, whereas Pb and Sr show correlation with
7
8 uranium-unsupported samples. Leachable elements that correlate with uranium in
9
10 uranium-supported radiogenic Pb samples from outside Zone K are Ca, Ni, Pb, Sr and Zr,
11
12 while the leachable elements that correlate with uranium in uranium-unsupported samples
13
14 are Ca, Co, Ni, Sr and Th.
15
16
17

18
19 Pb leached from the mineralized sample REA106-558.5, which is 5 km away
20
21 from the McArthur River uranium deposit, has a high $^{206}\text{Pb}/^{204}\text{Pb}$ ratio of 1141 with
22
23 uranium-supported Pb. The leach has a $^{207}\text{Pb}/^{206}\text{Pb}$ age of 1109 Ma, younger than the
24
25 1590 Ma main mineralization event in Athabasca Basin (Alexandre et al. 2009) and
26
27 younger than the other samples from the Wheeler River area. Leachable elements that are
28
29 enriched in the mineralized sample include Ag, As, Ba, Co, Ni, Pb, Sr, Th, Zn and Zr.
30
31
32
33
34
35
36

37 **Discussion**

38 *Nature and sequence of the alteration fluids*

39
40
41 The Ca-Sr-rich nature of early hydrothermal alteration substage APS1 goyazite is
42
43 consistent with formation from alteration of detrital apatite by basinal fluids, as detrital
44
45 apatite is commonly found in the Manitou Falls Formation whereas basement rocks are
46
47 generally enriched in REE and Th compared to the Manitou Falls Formation (Hecht and
48
49 Cuney, 2000). The Ca-Sr-rich nature of APS1 goyazite therefore suggests that basinal
50
51 fluids were responsible for both Ms1 muscovite and APS1 goyazite formation at a
52
53 minimum age of 1548 Ma (Fig 15a), as C1 sudoite from the mid hydrothermal stage was
54
55 present at that time.
56
57
58
59
60
61
62
63
64
65

1
2
3
4 Mid hydrothermal alteration substage C1 sudoite precipitated from fluids
5
6 isotopically similar to the early hydrothermal alteration substage basinal fluids that
7
8 formed Ms1 muscovite, but at lower temperatures near 175°C. However, the Mg needed
9
10 to precipitate C1 sudoite could not be derived from the preserved detrital minerals present
11
12 in the Manitou Falls Formation, suggesting infiltration of basinal fluids into the basement
13
14 rocks to acquire Mg (Fig. 15b). These chemically modified fluids were then reinjected
15
16 into the basal 200 meters of the Manitou Falls Formation precipitating dravite and
17
18 sudoite. At Zone K, late hydrothermal alteration substage C2 clinocllore precipitated
19
20 from basement fluids (Fig 15c) with lower $\delta^{18}\text{O}$ than the basinal fluids identified for the
21
22 previous hydrothermal alteration phases (Fig. 11) and at temperatures around 230°C. The
23
24 presence of LREE-Th-rich APS2 florencite and copper sulfides precipitating
25
26 simultaneously with C2 clinocllore is consistent with leaching of monazite in the reduced
27
28 basement rocks. Moreover, the higher precipitation temperature of C2 clinocllore, APS2
29
30 florencite and copper sulfides relative to C1 chlorite reflects a deeper source than the
31
32 source of the fluids that precipitated C1 sudoite, also supporting a basement origin. This
33
34 fluid not only precipitated the small quantities of C2 chlorite, but it also partially altered
35
36 the C1 chlorite.

37
38 The isotopic compositions of the fluids in equilibrium with post hydrothermal
39
40 alteration stage K2 kaolinite are not consistent with basin- or basement-derived fluids
41
42 previously reported in other studies (Wilson and Kyser, 1987; Kotzer and Kyser, 1995)
43
44 and plot close to the meteoric water line. Instead, the isotopic compositions of these
45
46 fluids are similar to kaolinite which formed from meteoric waters near 50°C, and are also
47
48 similar to the values obtained on post hydrothermal alteration stage kaolinite by Kotzer
49
50
51
52
53
54
55
56
57
58
59
60
61
62
63
64
65

1
2
3
4 and Kyser (1995) and Alexandre et al. (2005), which were interpreted to be related to
5
6 meteoric water incursion in faults and fractures since the Cretaceous (Fig. 15d).
7
8

9
10 *Critical factors revealed at the Zone K alteration system*
11

12
13 Paragenetic relationships, mineral chemistry, formation temperatures and mineral
14
15 isotopic compositions of the different alteration phases present at Zone K and other
16
17 sandstone-hosted unconformity-related uranium deposits in the Athabasca Basin are
18
19 similar, except for the presence of C2 clinochlore at Zone K (Kotzer and Kyser, 1995;
20
21 Fayek and Kyser, 1997; Kyser and Cuney, 2008). C2 clinochlore has a distinct chemistry
22
23 relative to other chlorites observed in the Manitou Falls Formation but is similar to pre-
24
25 mineralization chlorite found in basement-hosted deposits (Alexandre et al., 2005).
26
27

28
29 However, the basement fluids that formed the C2 clinochlore were reducing and a
30
31 sandstone-hosted deposit would be expected if these fluids mixed with oxidized basinal
32
33 fluids. The critical factor between Zone K and other sandstone-hosted unconformity-
34
35 related uranium deposits is the temporal relationship between the different fluids. At
36
37 Zone K, the uranium-bearing oxidized basinal fluids were not present to mix with
38
39 reduced chemically modified basinal fluids during the mid hydrothermal substage and
40
41 with reduced basement fluids during the late hydrothermal substage as reflected by
42
43 paragenetic relationships and chemical overprint of Ms1 muscovites by mid hydrothermal
44
45 substage C1 sudoite and late hydrothermal substage C2 clinochlore (Fig. 6a, 11). In
46
47 contrast, uranium-bearing oxidized basinal fluids in sandstone-hosted unconformity-
48
49 related uranium deposits of the Athabasca Basin were present to interact with reducing
50
51 fluids (Wilson and Kyser, 1987; Kotzer and Kyser, 1995; Fayek and Kyser, 1997;
52
53 Jefferson et al., 2007), thereby precipitating uranium. Unless a significant amount of both
54
55
56
57
58
59
60
61
62
63
64
65

1
2
3
4 oxidizing and reducing fluids were present simultaneously, uranium does not precipitate
5
6 despite the formation of alteration minerals.
7
8
9

10
11 *Application to exploration*
12
13

14
15 Low amounts of uranium-unsupported radiogenic Pb in the Athabasca Group at
16
17 Zone K, and a Pb-Pb model age of 1907 ± 140 Ma (Fig. 14), which is older than the 1590
18
19 Ma main mineralization event in the Athabasca Basin (Alexandre et al, 2009), indicate a
20
21 low potential for a sandstone-hosted uranium deposit in this area. Correlation between
22
23 Ca, P, Pb and Sr in uranium-supported samples at Zone K also supports a low potential
24
25 for uranium deposits, as the source for the uranium (and Pb) contained in the leachates is
26
27 likely from detrital apatite. However, our results do not exclude the possible presence of a
28
29 basement-hosted uranium deposit below Zone K. This is because low amounts of
30
31 radiogenic Pb and an old Pb-Pb model age of 2875 Ma occur in the Manitou Falls
32
33 Formation above the Millennium basement-hosted deposit, even though high amounts of
34
35 radiogenic Pb with a young Pb-Pb model age of 1075 ± 400 Ma are observed in the
36
37 basement (Cloutier et al., 2009). At Millennium, radiogenic Pb did not infiltrate the
38
39 Manitou Falls Formation above the deposit (Cloutier et al., 2009).
40
41
42
43
44
45

46
47 The leachates from outside Zone K indicate a greater influence from nearby
48
49 uranium deposits as reflected by high radiogenic Pb contents and uranium present in
50
51 uranium-unsupported samples correlating with Ca, Co, Ni, Sr, and Th. Provenance of the
52
53 radiogenic Pb in drill hole REA106 is most likely the McArthur River deposit, which is 5
54
55 km away. The source for the radiogenic Pb in drill holes WR188, WR189 and WR190A
56
57 could also be the McArthur River deposit but these are 20.5 to 29.8 km from the deposit.
58
59
60
61
62
63
64
65

1
2
3
4 Holk et al. (2003) observed radiogenic Pb migration along the unconformity only up to 8
5
6 km away from the McArthur River deposit, which would suggest that the high ratios in
7
8 drill holes WR188, WR189 and WR190A are related to more proximal mineralization.
9
10 The high amounts of radiogenic Pb observed near the unconformity in drill hole WR190A
11
12 may be related to the high grade uranium of up to 62.6% U₃O₈ over 6.0 meters
13
14 intersected by Denison Mines Corp in a drill hole 200 meters from WR190A (Press
15
16 release by Denison Mines Corp, August 12, 2009). Another possible source for the
17
18 radiogenic Pb is the precipitation of minor amounts of uraninite in the sample because
19
20 minor amounts of C1 sudoite, derived from reduced chemically modified basinal fluids,
21
22 occur in a matrix of Ms1 muscovite, which was derived from oxidizing basinal fluids.
23
24 The area outside Zone K with the best prospectivity is near drill hole WR188. Samples
25
26 from this drill hole record both oxidizing (Ms1 muscovite) and reducing (C1 sudoite)
27
28 fluids, the presence of radiogenic Pb and the correlation of pathfinder elements (Co and
29
30 Ni) with uranium.
31
32
33
34
35
36
37

38 The chemical compositions of APS minerals from sandstone- and basement-
39
40 hosted deposits of the Athabasca Basin have been proposed as a vector to mineralization
41
42 (Gaboreau et al., 2007). APS minerals with higher LREE and Th are found closer to a
43
44 uranium deposit whereas APS minerals with higher Sr and Ca represent a more distal
45
46 zone. The chemical composition of APS1 goyazite at Zone K would correspond to
47
48 proximal to intermediate alteration zone in the Athabasca Group (Fig. 7), whereas APS2
49
50 florencite is similar to those reported in the proximal alteration zone of basement-hosted
51
52 deposits (Gaboreau et al., 2007; Fig. 7). As an alternative to the APS chemistry reflecting
53
54 the relative distance to a uranium deposit, we propose that the chemistry of the APS
55
56
57
58
59
60
61
62
63
64
65

1
2
3
4 minerals reflect the source of the fluid, wherein APS1 goyazite reflects leaching of
5
6 Manitou Falls Formation detrital apatite by oxidized basinal fluids and APS2 florencite is
7
8 leaching of monazite from granitic rocks in the basement.
9

10
11 Laverret et al. (2006) proposed a vector to mineralization at Shea Creek using
12
13 different polytypes of muscovite in the Manitou Falls Formation. They suggested that the
14
15 1Mc polytype reflects regional alteration from basinal brines whereas the 1Mt polytype is
16
17 related to modified basinal brines that formed after interaction with basement rocks in the
18
19 vicinity of a mineralized area. However, the chemistry of this modified basinal brine
20
21 would likely be buffered by dravite and sudoite based on mineral paragenesis. At the
22
23 Wheeler River area, we interpret the 1Mt polytype to be associated with post-
24
25 hydrothermal alteration fluid movement along the unconformity and in brittle fractures,
26
27 sometimes associated with mineralized areas, but not related to the mineralizing fluids.
28
29 This is supported by petrographic observations wherein the 1Mt polytype is
30
31 paragenetically late and not related to sudoite, by the lack of leachable radiogenic Pb in
32
33 the Wheeler River area and by the presence of late kaolinite that indicate late fluids had
34
35 access to some parts of the Wheeler River area. In contrast to Shea Creek, the polytype of
36
37 muscovite is not an indicator of mineralization in the Wheeler River area.
38
39
40
41
42
43
44
45
46
47
48

49 **Conclusions**

50
51 Alteration mineral assemblages in Zone K of the Wheeler River area are similar to
52
53 those in mineralized systems, but detailed petrographic observations differentiate them.
54
55 The alteration present at the Wheeler River area consists of diagenetic dickite followed
56
57 by early hydrothermal alteration substage 1Mc muscovite and goyazite precipitating from
58
59
60
61
62
63
64
65

1
2
3
4 basinal fluids at temperatures of ca. 240°C and at a minimum age of 1548 ± 23 Ma.
5
6 Interaction of basinal fluids with the underlying basement rocks produced chemically
7
8 distinct Mg-rich basinal fluids, which were reinjected into the basal 200 meters of the
9
10 Manitou Falls Formation after the basinal fluids waned, and precipitated dravite and
11
12 sudoite at temperatures of 175°C and at a maximum age of 1548 ± 23 Ma. At Zone K,
13
14 later basement fluids with lower $\delta^{18}\text{O}$ values and different chemical compositions than
15
16 the basinal brines in the Manitou Falls Formation produced a ~250 meters high by ~250
17
18 meters wide clinocllore, copper sulfides and florencite halo in the basal portion of the
19
20 Manitou Falls Formation at temperatures around 230°C, but the lack of significant
21
22 basinal fluids at that time prevented the precipitation of uraninite.
23
24
25
26
27
28

29 Thus, the low potential for a sandstone-hosted deposit in Zone K is attributed to the
30
31 relative timing of the fluid circulation events, with uranium-bearing basinal fluids being
32
33 present prior to basement reducing fluids, which precluded uranium precipitation in the
34
35 sandstone. The low probability for a sandstone-hosted uranium deposit at Zone K is
36
37 supported by low amounts of radiogenic Pb and by a Pb-Pb model age of 1907 Ma that is
38
39 older than the Athabasca Basin. Prospective areas of possible unconformity-related
40
41 uranium deposits were identified outside Zone K near drill hole WR188, WR189 and
42
43 WR190A using the weak acid leach technique wherein significant amounts of uranium-
44
45 unsupported radiogenic Pb were observed.
46
47
48
49
50
51
52

53 **Acknowledgements**

54
55
56 This work benefited from financial support from the Natural Sciences and
57
58 Engineering Research Council of Canada (NSERC) Collaborative Research &
59
60
61
62
63
64
65

1
2
3
4 Development program and Discovery Grant program as well as from field and financial
5 support from Cameco Corporation. Leigh Dauphin is thanked for his field support. Kerry
6
7 Klassen, Don Chipley, April Vuletich and Bill MacFarlane are thanked for help with
8
9 stable and radiogenic isotope analyses at the Queen's University Facility for Isotope
10
11 Research. Peter Jones was instrumental with the SEM and electron microprobe analyses
12
13 at Carleton University, Ottawa. Dan Jiricka, Roger Wallis and Paul Ramaekers are
14
15 thanked for reviewing this manuscript and for their insightful comments, and Larry
16
17 Meinert for his editorial work.
18
19
20
21
22
23
24
25

26 **References**

- 27
28
29 Alexandre P., Kyser K., Polito P., and Thomas D., 2005, Alteration Mineralogy and
30
31 Stable Isotope Geochemistry of Paleoproterozoic Basement-Hosted Unconformity-
32
33 Type Uranium Deposits in the Athabasca Basin, Canada: Economic Geology, v.100-8,
34
35 p.1547-1563.
36
37
38
39
40 Alexandre P., Kyser K., Thomas D., Polito P., and Marlat J., 2009, Geochronology of
41
42 unconformity-related uranium deposits in the Athabasca Basin, Saskatchewan,
43
44 Canada, and their integration in the evolution of the basin: Mineralium Deposita, v.44-
45
46 1, 41-59.
47
48
49
50
51 Annesley, I.R., Madore, C., and Portella, P., 2005, Geology and thermotectonic evolution
52
53 of the western margin of the Trans-Hudson Orogen: evidence from the eastern sub-
54
55 Athabasca basement, Saskatchewan: Canadian Journal of Earth Sciences, v.42, p.573-
56
57 597.
58
59
60
61
62
63
64
65

- 1
2
3
4 Armstrong R.L., and Ramaekers, P., 1985, Sr isotopic study of the Helikian sediment and
5
6 diabase dikes in the Athabasca Basin, northern Saskatchewan: Canadian Journal of
7
8 Earth Sciences, v.22, p.399-407.
9
10
11
12 Awwiler, D.N., 1993, Illite/smectite formation and potassium mass transfer during burial
13
14 diagenesis of mudrocks: A study from the Texas Gulf Coast Paleocene-Eocene:
15
16 Journal of Sedimentary Petrology, v.63-3, p.501-512.
17
18
19
20 Bailey, S.W., 1980, Summary of recommendations of AIPEA nomenclature committee
21
22 on clay minerals: American mineralogist, v.65, p.1-7.
23
24
25
26 Billault, V., Beaufort, D., Patrier, P., and Petit, S., 2002, Crystal chemistry of Fe-sudoites
27
28 from uranium deposits in the Athabasca Basin (Saskatchewan, Canada): Clays and
29
30 clay minerals, v.50-1, 70-81.
31
32
33
34 Burwash, R.A., Baadsgaard, H., and Peterman, Z.E., 1962, Precambrian K-Ar dates from
35
36 the Western Canada sedimentary basin: Canadian Journal of Earth Sciences, v.29,
37
38 p.879-895.
39
40
41
42 Cathelineau, M., 1988, Cation site occupancy in chlorites and illites as a function of
43
44 temperature: Clay Minerals, v.23, p.471-485.
45
46
47
48 Clayton, R.N., and Mayeda, T.K., 1963, The use of bromine pentafluoride in the
49
50 extraction of oxygen from oxides and silicates for isotopic analysis: Geochimica et
51
52 Cosmochimica Acta, v.27, p.43-52.
53
54
55
56 Cloutier, J., Kyser, K., Olivo, G.R., Alexandre, P., and Halaburda, J., 2009, The
57
58 Millennium uranium deposit, Athabasca Basin, Saskatchewan, Canada: An atypical
59
60
61
62
63
64
65

1
2
3
4 basement-hosted unconformity-related uranium deposit: *Economic Geology*, v.104,
5
6 p.815-840.
7
8

9
10 Cumming, G.I., and Krstic, D., 1992, The age of unconformity uranium mineralization in
11
12 the Athabasca Basin, northern Saskatchewan: *Canadian Journal of Earth Sciences*,
13
14 v.29, p.1623-1639.
15
16

17
18 Deer, W.A., Howie, R.A., and Zussman, J., 1992, An introduction to rock-forming
19
20 minerals: London, Longman, 696p.
21
22

23
24 Drits, V.A., Weber, F., Salyn, A.L., and Tsipurski, S.I., 1993, X-Ray identification of
25
26 one-layer varieties: application to the study of illites around uranium deposits of
27
28 Canada: *Clays and clay minerals*, v.41-3, p.389-398.
29
30

31
32 Earle, S., and Sopuck, V., 1989, Regional lithogeochemistry of the eastern part of the
33
34 Athabasca Basin uranium province, Saskatchewan: In Miller-Kahle, ed., *Uranium*
35
36 *resources and geology of North America*. International Atomic Energy Agency,
37
38 Technical document TECHDOC-500, p.263-269.
39
40

41
42 Earle, S., Wheatley, K., and Wasyliuk, K., 1999, Application of reflectance spectroscopy
43
44 to assessment of alteration mineralogy in the Key Lake area: *MinExpo'96 – Advances*
45
46 *in Saskatchewan geology and mineral exploration*, Saskatoon, November 21-22, 1996,
47
48 *Proceedings*, 109-123.
49
50

51
52 Fayek, M., and Kyser, K., 1997, Characterization of multiple fluid-flow events and rare-
53
54 earth elements mobility associated with formation of unconformity uranium deposits
55
56 in the Athabasca basin, Saskatchewan: *Canadian Mineralogist*, v.35, p.627-658.
57
58
59
60
61
62
63
64
65

- 1
2
3
4 Gaboreau, S., Cuney, M., Quirt, D., Beaufort, D., Patrier, P., and Mathieu, R., 2007,
5
6 Significance of aluminum phosphate-sulfate minerals associated with U unconformity-
7
8 type deposits: The Athabasca basin, Canada: *American Mineralogist*, v.92, p.267-280.
9
10
11
12 Hecht, L., and Cuney, M., 2000, Hydrothermal alteration of monazite in the Precambrian
13
14 crystalline basement of the Athabasca Basin (Saskatchewan, Canada): implications for
15
16 the formation of unconformity-related uranium deposits: *Mineralium Deposita*, v.35,
17
18 p.791-795.
19
20
21
22
23 Hoeve, J., and Quirt, D.H., 1984, Mineralization and host rocks alteration in relation to
24
25 clay mineral diagenesis and evolution of the Middle-Proterozoic, Athabasca Basin,
26
27 northern Saskatchewan, Canada: Saskatchewan Research Council, SRC Technical
28
29 Report 187, 187p.
30
31
32
33
34 Hoeve, J., and Sibbald, T.I.I., 1978, On the genesis of Rabbit Lake and other
35
36 unconformity-type uranium deposits in northern Saskatchewan, Canada: *Economic*
37
38 *Geology*, v.73, p.1450-1473.
39
40
41
42 Hoffman, P.F., 1988, United Plates of America, the birth of a craton: Early Proterozoic
43
44 assembly and growth of Laurentia: *Annual Review of Earth and Planetary Sciences*,
45
46 v.16, p.543-603.
47
48
49
50 Holk, G., Kyser, T.K., Chipley, D., Hiatt, E., and Marlat, J., 2003, Mobile Pb-isotopes in
51
52 Proterozoic sedimentary basins as guides for exploration of uranium deposits: *Journal*
53
54 *of Geochemical Exploration*, v.80, p.297-320.
55
56
57
58
59
60
61
62
63
64
65

1
2
3
4 Jefferson, C.W., Thomas, D.J., Gandhi, S.S., Ramaekers, P., Delaney, G., Brisbin, D.,
5
6 Cutts, C., Portella, P., and Olson, R.A., 2007, Unconformity-associated uranium
7
8 deposits of the Athabasca Basin, Saskatchewan and Alberta: in Jefferson C.W. and
9
10 Delaney G. (editors) EXTECH IV: Geology and Uranium EXploration TECHnology
11
12 of the Proterozoic Athabasca Basin, Saskatchewan and Alberta, Geological Survey of
13
14 Canada Bulletin 588, Saskatchewan Geological Society Special Publication 18,
15
16
17
18 Mineral Deposit Division (GAC) special publication 4, p.23-67.
19
20
21

22 Kotzer, T.G., and Kyser, T.K., 1995, Petrogenesis of the Proterozoic Athabasca Basin,
23
24 northern Saskatchewan, and its relation to diagenesis, hydrothermal uranium
25
26 mineralization and paleohydrology: *Chemical Geology*, v.120, p.45–89.
27
28
29

30 Krasenberg, H.J., 2004, The Newest gold: uranium: European Gold Center, oct 10, p.1-3.
31
32

33
34 Kyser, K., and Cuney, M., 2008, Unconformity-related uranium deposits, in Cuney, M.
35
36 and Kyser, K., Recent and not-so-recent developments in uranium deposits and
37
38 implications for exploration, Mineralogical Association of Canada Short Course 39,
39
40 p.161-219.
41
42
43

44 Kyser, K., Hiatt, E., Renac, C., Durocher, K., Holk, G., and Deckart, K., 2000,
45
46 Diagenetic fluids in Paleo- and Meso-Proterozoic sedimentary basins and their
47
48 implications for long protracted fluid histories, in Kyser, T.K., ed., *Fluids and Basin*
49
50 *Evolution: Mineralogical Association of Canada Short Course 28*, p. 225-262.
51
52
53
54

55 Laverret, E., Mas, P.P., Beaufort, D., Kister, P., Quirt, D., Bruneton, P., and Norbert, C.,
56
57 2006, Mineralogy and geochemistry of the host-rock alterations associated with the
58
59 Shea Creek unconformity-type uranium deposits (Athabasca Basin, Saskatchewan,
60
61
62
63
64
65

1
2
3
4 Canada). Part.1 Spacial variation of illite properties: Clays and Clay Minerals, v.54-3,
5
6 p.275-294.
7
8
9

10 LeCheminant, A.N., and Heaman, L.M., 1989, Mackenzie igneous events, Canada:
11
12 Middle Proterozoic hotspot magmatism associated with ocean opening: Earth and
13
14 Planetary Science Letters, v.96, p.38-48
15
16
17

18 Lewry ,J.F., and Sibbald, T.I.I., 1980, Thermotectonic evolution of the Churchill
19
20 province in northern Saskatchewan: Tectonophysics, v.68, p.45-82.
21
22
23

24 Ludwig, K.R., 2000, Isoplot/Ex. A geochronological toolkit for Microsoft Excel:
25
26 Berkeley Geochronology Center Special publication no. 1a, 53 p.
27
28
29

30 Marumo, N., Nagasawa, K., and Kuroda, Y., 1980, Mineralogy and hydrogen isotope
31
32 geochemistry of clay minerals in the Ohnuma geothermal area, northeastern Japan:
33
34 Earth and Planetary Science Letters, v.47, p.255-262.
35
36
37

38 McDougall, M., and Harrison, T.M., 1999, Geochronology and thermochronology by the
39
40 $^{39}\text{Ar}/^{40}\text{Ar}$ method: Oxford University Press, Oxford, 262p.
41
42
43

44 Nyman, M.W., Karlstrom, K.E., Kirby, E., and Graubard, C.M., 1994, Mesoproterozoic
45
46 contractional orogeny in North America: evidence from ca. 1.4 Ga plutons: Geology,
47
48 v.22, p.901-904.
49
50
51

52 O'Neil, J.R. and Taylor, H.P.Jr., 1969, Oxygen isotope equilibrium between muscovite
53
54 and water: Journal of Geophysical Research, v.74-25, p.6012-6022.
55
56
57
58
59
60
61
62
63
64
65

1
2
3
4 Pacquet, A., and Weber, B., 1993, Pétrographie et minéralogie des halos d'altération
5
6
7 autour du gisement de Cigar Lake et leurs relations avec les minéralisations: Canadian
8
9 Journal of Earth Sciences, 30, 674-688.

10
11
12 Pagel, M., Poty, B., and Sheppard, S.M.F., 1980, Contribution to some Saskatchewan
13
14 uranium deposits mainly from fluid inclusions and isotopic data: In Ferguson, S. and
15
16 Goleby, A., eds., Uranium in the Pine Creek Geosyncline. Vienna, International
17
18 Atomic Energy Agency, 639-654.

19
20
21
22
23 Percival, J.B., Bell, K., Torrance, J.K., 1993, Clay mineralogy and isotope geochemistry
24
25 of the alteration halo at the Cigar Lake uranium deposit: Canadian Journal of Earth
26
27 Sciences, V.30, p.689-704.

28
29
30
31 Quirt, D.H., 2003, Athabasca unconformity-type uranium deposits: one deposit type with
32
33 many variations: Uranium Geochemistry 2003, International Conference, Nancy,
34
35 France, April 13-16, 2003, Proceedings, p.309-312.

36
37
38
39 Quirt, D.H., and Wasyliuk, K., 1997, Kaolinite, dickite, and other clay mineral in the
40
41 Athabasca Group, Canada and the Kombolgie Formation, Australia: 11th International
42
43 Clay Conference, Ottawa, Ontario, June 1997, Proceedings, A61.

44
45
46
47 Ramaekers, P., 1990, Geology of the Athabasca Group (Helikian) in Northern
48
49 Saskatchewan: Saskatchewan Energy and Mines, Saskatchewan Geological Survey
50
51 Report 195, 48 p.

1
2
3
4 Ramaekers, P., and Dunn, C.E., 1977, Geology and geochemistry of the eastern margin
5 of the Athabasca Basin. in Dunn, C.E., ed., Uranium in Saskatchewan: Saskatchewan
6 Geological Survey Special Publication 3, p.297-322.
7
8
9

10
11
12 Ramaekers, P., Jefferson, C.W., Yeo, G.M., Collier, B., Long, D.G.F., Grever, S.,
13
14 McHardy, S., Jiricka, D., Cutts, C., Wheatley, K., Catuneanu, O., Bernier, S., Kupsch,
15
16 B., and Post, R.T., 2007, Revised geological map and stratigraphy of the Athabasca
17
18 Group, Saskatchewan and Alberta: in Jefferson C.W. and Delaney G. (editors)
19
20 EXTECH IV: Geology and Uranium EXploration TECHnology of the Proterozoic
21
22 Athabasca Basin, Saskatchewan and Alberta, Geological Survey of Canada Bulletin
23
24 588, Saskatchewan Geological Society Special Publication 18, Mineral Deposit
25
26 Division (GAC) special publication 4, p.155-191.
27
28
29
30
31

32
33 Renac, C., Kyser, T.K., Durocher, K., Dreaver, G., O'Connor, T., 2002, Comparison of
34
35 diagenetic fluids in the Proterozoic Thelon and Athabasca Basins, Canada:
36
37 implications for protracted fluid histories in stable intracratonic basins: Canadian
38
39 Journal of Earth Sciences, 39, p.113-132.
40
41
42

43 Sheppard, S.M.F., and Gilg, H.A., 1996, Stable isotope geochemistry of clay minerals:
44
45 Clay minerals, v.31, p.1-24.
46
47
48

49 Sibbald, T.I.I., and Quirt, D., 1987, Uranium deposits of the Athabasca basin:
50
51 Saskatchewan Research Council Publication R-855-1-G-87, 79p.
52
53
54

55 Sims, P.K., and Stein, H.J., 2001, Tectonic history of the Proterozoic Colorado Province,
56
57 Southern Rocky Mountains: Abstract with Programs Geological Society of America,
58
59 33-5, p.4.
60
61
62

- 1
2
3
4 Thomas, D.J., Matthews, R.B., and Sopuck, V.J., 1998, Athabasca Basin unconformity-
5
6 type uranium deposits: a synopsis of the empirical model and review of exploration
7
8 and production trends: Proceedings, Canadian Institute of Mining, Metallurgy and
9
10 Petroleum meeting, Montreal 1998, May 3-7.
11
12
13
14
15 Thomas, D., 2000, Comparison of mesoscopic structural and alteration features in
16
17 basement and sandstone, Zone K, Wheeler River Project: Unpublished report by
18
19 Cameco Corporation, 31p.
20
21
22
23 Tran, H.T., Ansdell, K., Bethune, K., Watters, B., and Ashton, K., 2003, Nd isotope and
24
25 geochemical constraints on the depositional setting of Paleoproterozoic
26
27 metasedimentary rocks along the margin of the Archean Hearne craton, Saskatchewan,
28
29 Canada: Precambrian Research, v.123, p.1-28.
30
31
32
33
34 Vennemann, T.W., and O'Neil, J.R., 1996, Hydrogen isotope exchange reactions
35
36 between hydrous minerals and molecular hydrogen: I. A new approach for the
37
38 determination of hydrogen isotope fractionation at moderate temperatures:
39
40 Geochimica et Cosmochimica Acta, v.60-13, p.2437-2451.
41
42
43
44 Wasyliuk, K., 2002, Petrogenesis of the kaolinite-group minerals in the eastern
45
46 Athabasca Basin of northern Saskatchewan: Applications to uranium mineralization:
47
48 Msc thesis, University of Saskatchewan, Saskatoon, Saskatchewan, 140p.
49
50
51
52
53 Wenner, D.B., and Taylor, H.P. Jr., 1971, Temperature of serpentinization of ultramafic
54
55 rocks based on O^{18}/O^{16} fractionation between coexisting serpentinite and magnesite:
56
57 Contributions to Mineralogy and Petrology, v.32, p.165-185.
58
59
60
61
62
63
64
65

1
2
3
4
5
6
7
8
9
10
11
12
13
14
15
16
17
18
19
20
21
22
23
24
25
26
27
28
29
30
31
32
33
34
35
36
37
38
39
40
41
42
43
44
45
46
47
48
49
50
51
52
53
54
55
56
57
58
59
60
61
62
63
64
65

Wilson, M.R., and Kyser, K., 1987, Stable isotopes geochemistry of alteration associated with the Key Lake uranium deposit, Canada: *Economic Geology*, v.82, p.1540–1557.

Yeh, H-W., 1980, D/H ratios and late-stage dehydration of shale's during burial: *Geochimica et Cosmochimica Acta*, v.44, p341-352.

1
2
3
4 **Figure Captions**
5
6

7
8 Figure 1: Simplified geologic map of the Athabasca Basin in northern Saskatchewan,
9
10 Canada. The major lithotectonic units of basement lithologies are indicated in *italics*.
11
12 Also shown is the position of the Wheeler River area (star) and major unconformity-
13
14 related uranium deposits (circle). BLSZ: Black Lake Shear Zone; VRSZ: Virgin River
15
16 Shear Zone. Modified after Sibbald and Quirt (1987).
17
18
19
20
21
22

23
24 Figure 2: Lithogeochemical map of the southeastern part of the Athabasca Basin after
25
26 Earle and Sopuck (1989) and Jefferson et al. (2007) showing regional illite, chlorite and
27
28 dravite anomalies. Also shown are the surface projected areas of the low magnetic
29
30 susceptibility in basement rocks (short bold dashed lines) and the location of buried
31
32 basement quartzite ridges (white bars). MF: Manitou Falls Formation; LZ: Lazenby Lake
33
34
35 Formation
36
37
38
39
40
41

42
43 Figure 3: (A) Schematic plan view of the location of the drill holes sampled. Samples
44
45 associated with Zone K are from drill holes ZK. (B) Schematic cross-section of the
46
47 Manitou Falls Formation of the Wheeler River area following a NNW-SSE transect and
48
49 (C) a SSW-NNE transect. Also shown on the cross-sections are the dominant alteration
50
51 minerals present, location of the drill holes sampled, and sample location.
52
53
54
55
56
57

58
59 Figure 4: General mineral paragenesis for Manitou Falls Formation in the Wheeler River
60
61
62
63
64
65

1
2
3
4 area. Three main stages of alteration are identified: diagenesis, hydrothermal alteration,
5
6 which is subdivided into an early, a mid and a late substage, and post hydrothermal
7
8 alteration. The thickness of the lines indicates the relative abundance. Dashed lines
9
10 indicate uncertainty in the position.
11
12
13
14
15
16

17 Figure 5: Photomicrographs of typical mineral assemblages in Manitou Falls Formation
18
19 related to diagenesis, hydrothermal alteration and post hydrothermal alteration events.
20

21 (A) Diagenetic H1 hematite coats a detrital Q0 quartz grain in H2 hematite matrix. (B)
22
23 Remnants of H2 hematite matrix showing embayments filled with diagenetic K1 dickite
24
25 and early hydrothermal alteration substage Ms1 muscovite. (C) Early hydrothermal
26
27 alteration substage Ms1 muscovite filling interstices in a K1 diagenetic dickite aggregate.
28
29 (D) Mid hydrothermal alteration substage C1 chlorite filling corroded zones in mid
30
31 hydrothermal alteration substage T1 dravite aggregates. (E) Late hydrothermal alteration
32
33 substage C2 chlorite vein crosscutting mid hydrothermal alteration substage C1 chlorite-
34
35 rich matrix. (F) Post hydrothermal alteration stage K2 kaolinite pseudomorphously
36
37 replacing late hydrothermal alteration substage C2 chlorite. XP: Cross-polar light.
38
39
40
41
42
43
44
45
46

47 Figure 6: (A) $\text{Si} + \text{Al}_{(\text{VI})} + \text{Mg} + \text{Fe}$ versus $\text{Al}_{(\text{IV})} + \text{K}$ for early hydrothermal alteration
48
49 substage Ms1_k muscovite (pale grey triangle) and Ms1_o muscovite (dark grey triangle)
50
51 showing a more variable composition for Ms1_k muscovite. Also shown is the field
52
53 occupied by Athabasca Basin sandstone-hosted uranium deposit white mica, referred to
54
55 as illite in previous publications (Wilson and Kyser, 1987; Pacquet and Weber, 1993;
56
57 Percival et al., 1993; Kotzer and Kyser, 1995; Alexandre et al., 2005). (B) SiO_2 - Al_2O_3 -
58
59
60
61
62
63
64
65

1
2
3
4 K₂O ternary diagram showing the composition of the Wheeler River area Ms1 muscovite,
5
6 C1 sudoite and C2 clinocllore. Also shown is the field of Athabasca Basin muscovite
7
8 (Wilson and Kyser, 1987; Pacquet and Weber, 1993; Percival et al., 1993; Kotzer and
9
10 Kyser, 1995; Alexandre et al., 2005) and ideal composition of dickite, dravite, K-feldpar,
11
12 illite and muscovite.
13
14
15
16
17
18
19

20
21 Figure 7: Plot of LREE+Th versus Sr+Ca for APS1 (square) and APS2 (diamond). Also
22
23 shown are the alteration fields of Gaboreau et al., (2007). Solid lines delineate basement-
24
25 hosted assemblages and dashed lines delineate sandstone-hosted assemblages.
26
27
28
29
30
31

32
33 Figure 8: Al-Mg-Fe ternary diagram for mid hydrothermal alteration substage C1 (grey
34
35 circle), late hydrothermal substage C2 (black circle) chlorites and chlorites with mixed
36
37 compositions (white circle) from Zone K of the Wheeler River area plotted as a function
38
39 of molar proportions (Bailey, 1980). The black solid line delineates the field of
40
41 sandstone-hosted chlorite while the dashed line delineates the field of pre-mineralization
42
43 chlorite reported in uranium deposit of the Athabasca Basement. (Wilson and Kyser,
44
45 1987; Pacquet and Weber, 1993; Kotzer and Kyser, 1995; Billault et al., 2002; Alexandre
46
47 et al., 2005). Also shown is the ideal composition of muscovite, clinocllore, sudoite and
48
49 the field of typical biotite (grey area) composition (Deer et al., 1992).
50
51
52
53
54
55
56
57
58
59
60
61
62
63
64
65

1
2
3
4 Figure 9: XRD profiles of early hydrothermal alteration substage Ms1 muscovites from
5 the Manitou Falls Formation at (A) Zone K and (B) outside Zone K. Muscovites from
6 Zone K (Ms1_k) represent a mixture between the 1Mc polytype and the 1Mt polytype,
7 while muscovites from outside Zone K (Ms1_o) are dominated by the 1Mc polytype. As
8 the unconformity is approached, samples from both zones record an increasing amount of
9 the 1Mt muscovite polytype. Peak position for 1Mc, 1Mt and 2M₁ muscovite polytypes
10 are from Drits et al. (1993).
11
12
13
14
15
16
17
18
19
20
21
22
23
24

25 Figure 10: Secondary Electron Scanning Electron Microscope microphotographs of (A)
26 detrital Q0 quartz, early hydrothermal alteration substage 1Mc (Ms1_k) muscovite from
27 Zone K with 1Mt (Ms2_k) muscovite overgrowth. (B) Early hydrothermal alteration
28 substage 1Mc (Ms1_k) muscovite from Zone K with 1Mt (Ms2_k) muscovite overgrowth.
29
30
31
32
33
34
35 (C) and (D) Early hydrothermal substage 1Mc (Ms1_o) muscovite from outside Zone K
36 with 1Mt (Ms2_o) muscovite overgrowth.
37
38
39
40
41
42
43

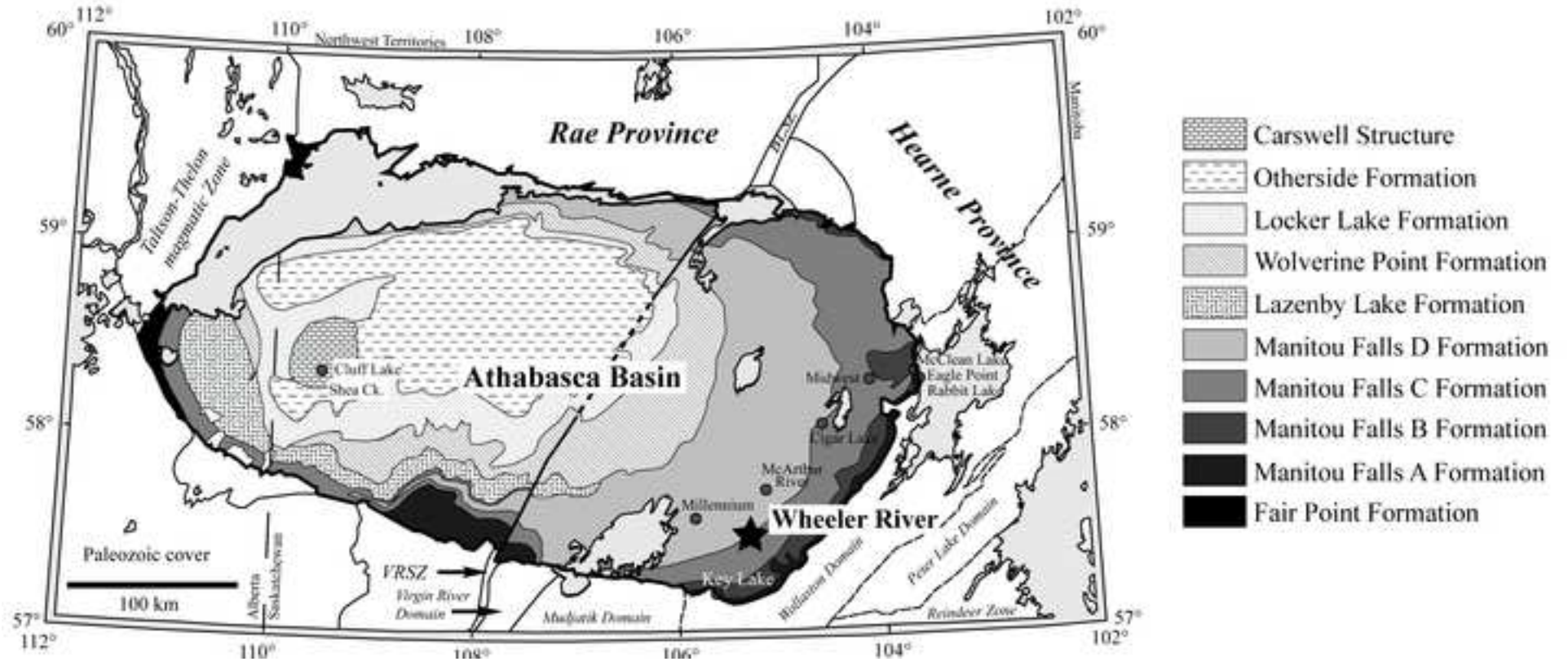
44 Figure 11: Calculated δD and $\delta^{18}O$ values of fluids in equilibrium with minerals from
45 various alteration stages from the Manitou Falls A, B, C and D Members. Also shown are
46 the meteoric water line (MWL) and the isotopic composition of Vienna standard mean
47 ocean water (V-SMOW).
48
49
50
51
52
53
54
55
56
57
58
59
60
61
62
63
64
65

1
2
3
4 Figure 12: $^{40}\text{Ar}/^{39}\text{Ar}$ spectra for (A) sample ZK13-202 showing a pseudo-plateau
5
6 $^{40}\text{Ar}/^{39}\text{Ar}$ age of 1497 ± 20 Ma on Ms1_k muscovite; (B) sample ZK16-320 showing a
7
8 pseudo-plateau $^{40}\text{Ar}/^{39}\text{Ar}$ age of 1237 ± 7 Ma on Ms1_k muscovite; (C) sample ZK18-464
9
10 showing a pseudo-plateau $^{40}\text{Ar}/^{39}\text{Ar}$ age of 1216 ± 6 Ma on Ms1_k muscovite; (D) sample
11
12 REA106-418 showing a pseudo-plateau $^{40}\text{Ar}/^{39}\text{Ar}$ age of 1356 ± 7 Ma on Ms1_o
13
14 muscovite; (E) sample WR189-421 showing a pseudo-plateau $^{40}\text{Ar}/^{39}\text{Ar}$ age of 1298 ± 7
15
16 Ma on Ms1_o muscovite and (F) sample ZK16-425 showing a plateau $^{40}\text{Ar}/^{39}\text{Ar}$ age of
17
18 1548.2 ± 22.8 Ma on C1_k chlorite.
19
20
21
22
23
24
25
26
27

28 Figure 13: Distribution of $^{206}\text{Pb}/^{204}\text{Pb}$ ratios from weak acid leached samples at Zone K
29
30 and outside Zone K along (A) a NNW-SSE transect and (B) a SSW-NNE transect. Also
31
32 shown is the dominant alteration mineral present, location of the drill holes sampled and
33
34 samples location. Dashed lines represent $^{206}\text{Pb}/^{204}\text{Pb}$ ratios between 30 and 50 and solid
35
36 lines represent $^{206}\text{Pb}/^{204}\text{Pb}$ ratios greater than 50.
37
38
39
40
41
42
43

44 Figure 14: $^{207}\text{Pb}/^{204}\text{Pb}$ versus $^{206}\text{Pb}/^{204}\text{Pb}$ isochron for Pb leached from samples from
45
46 Zone K giving a model age of 1907 ± 140 Ma.
47
48
49
50
51
52

53 Figure 15: Schematic model of the evolution of the fluids with the related alteration and
54
55 temperatures for Zone K of Wheeler River area based on paragenetic relationships and
56
57 isotopic compositions.
58
59
60
61
62
63
64
65



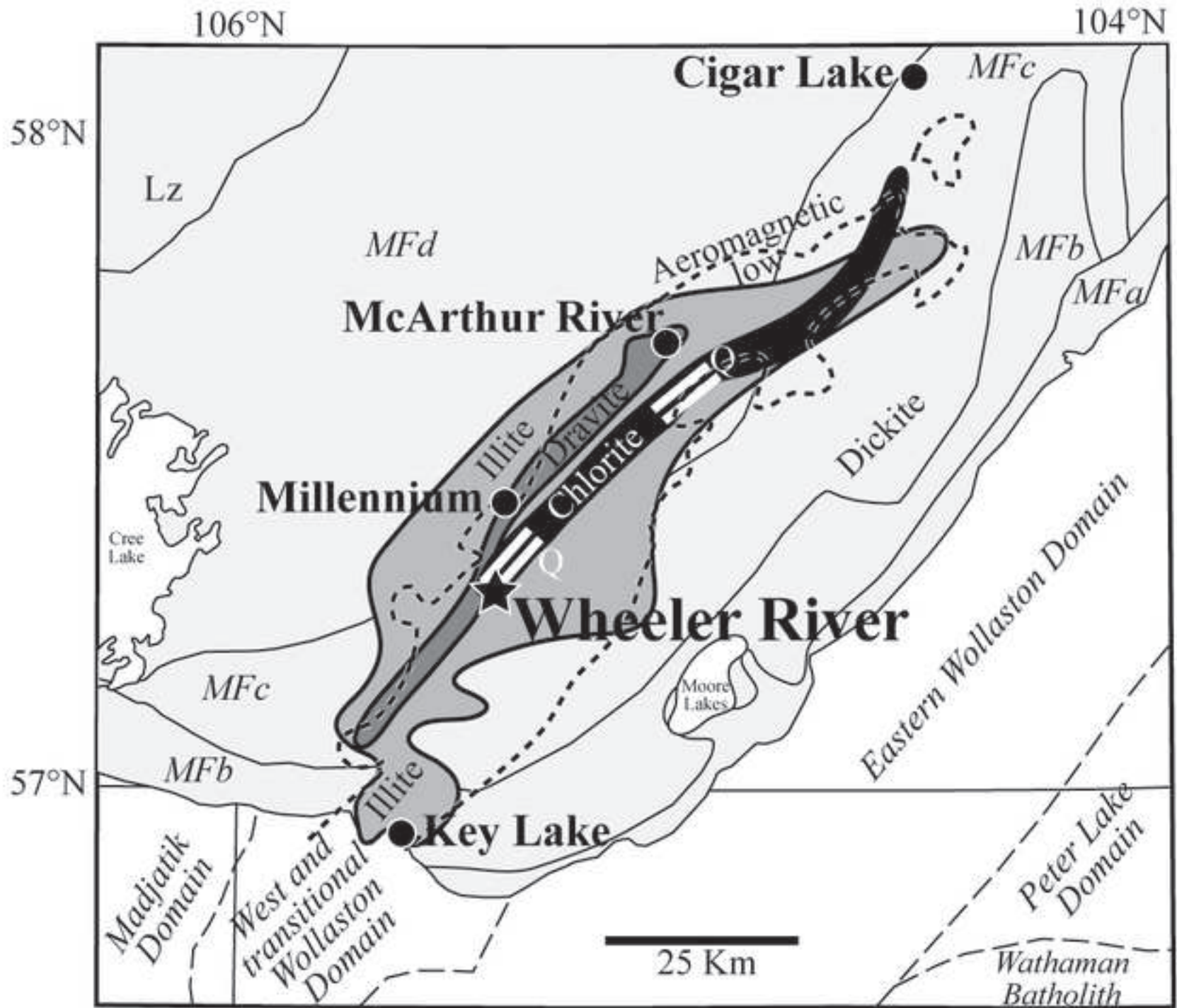
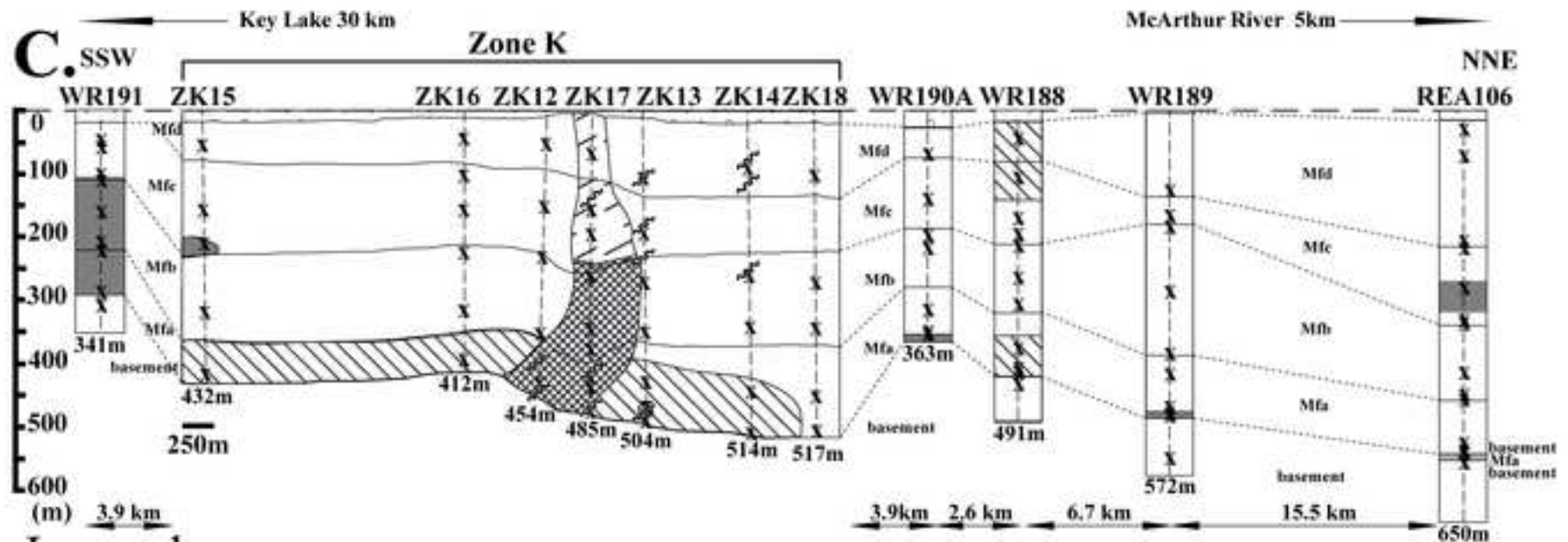
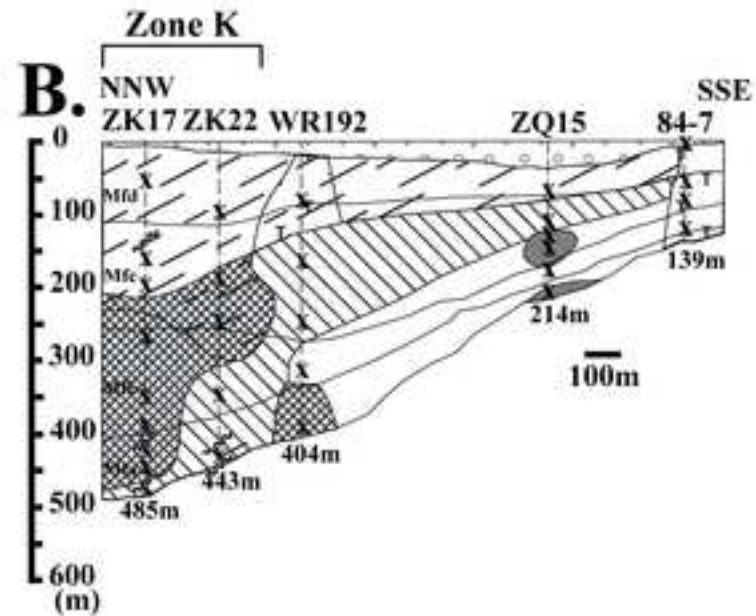
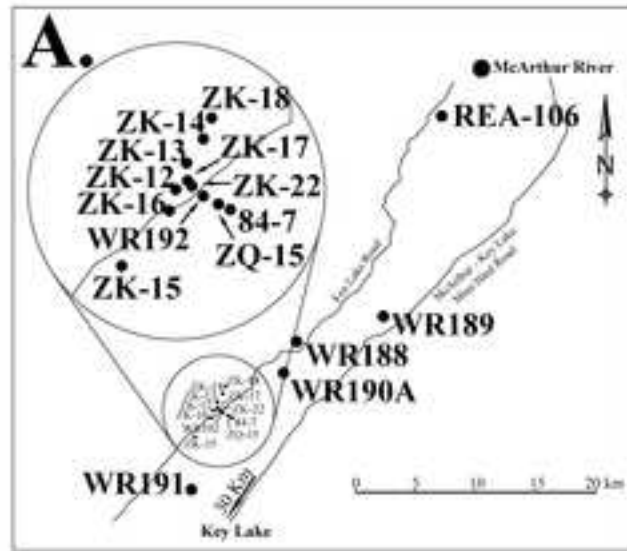


Figure 02



Legend



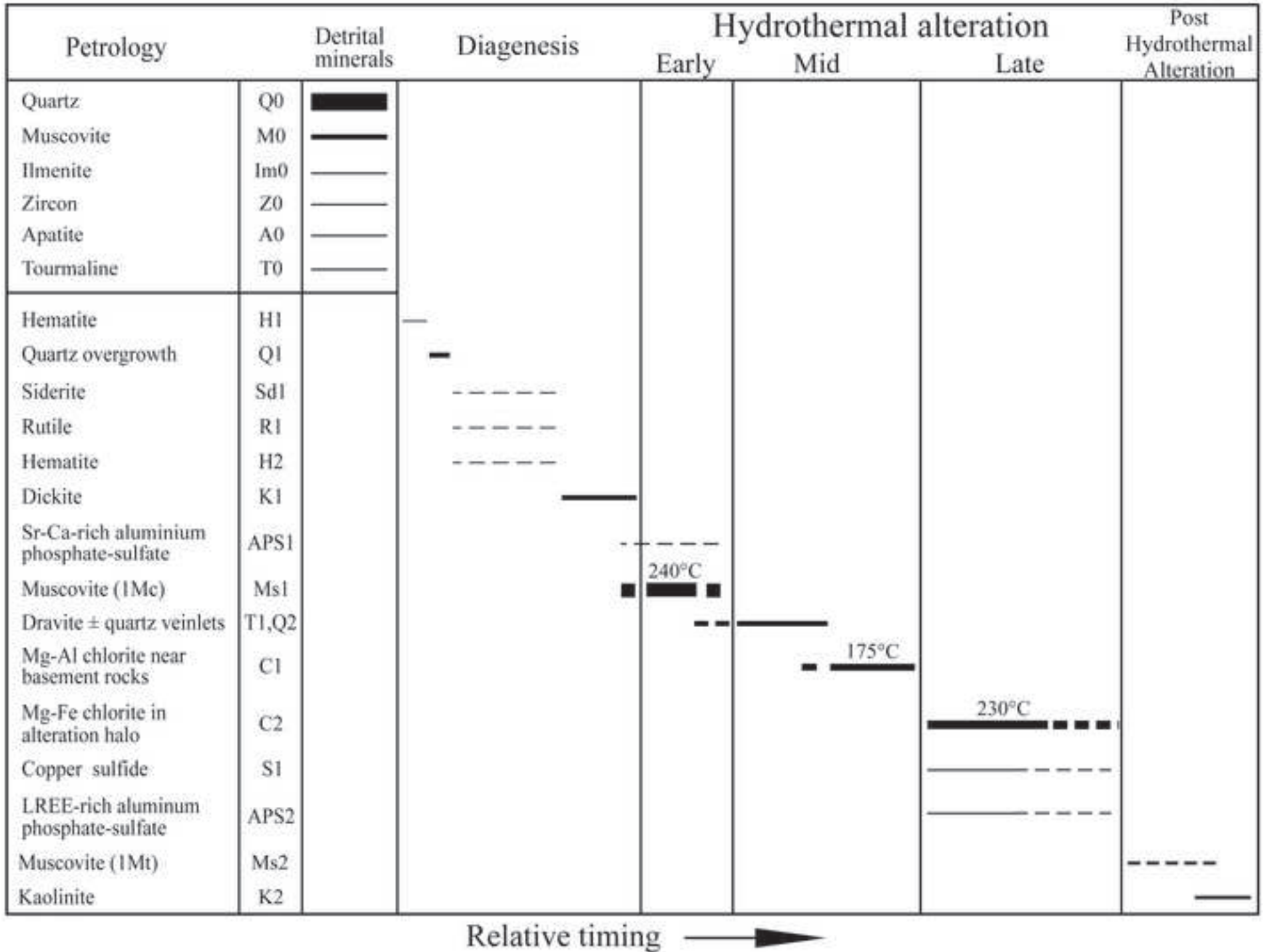


Figure 05

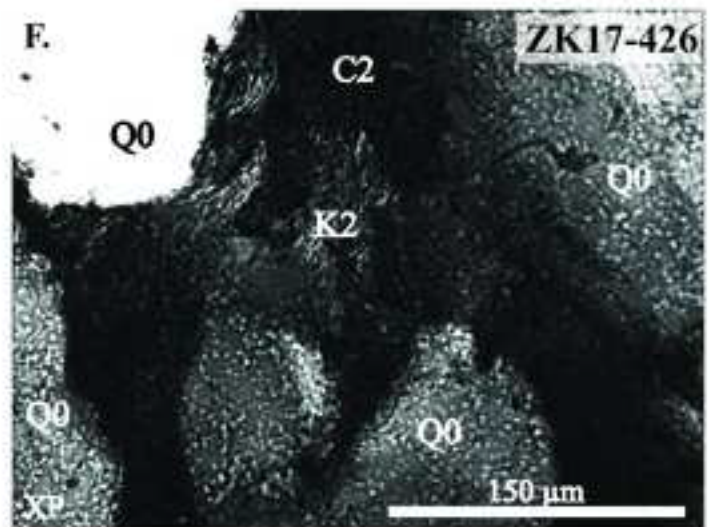
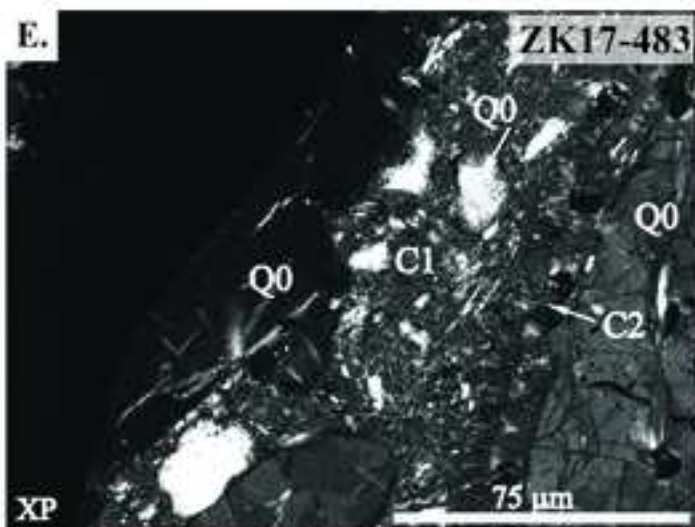
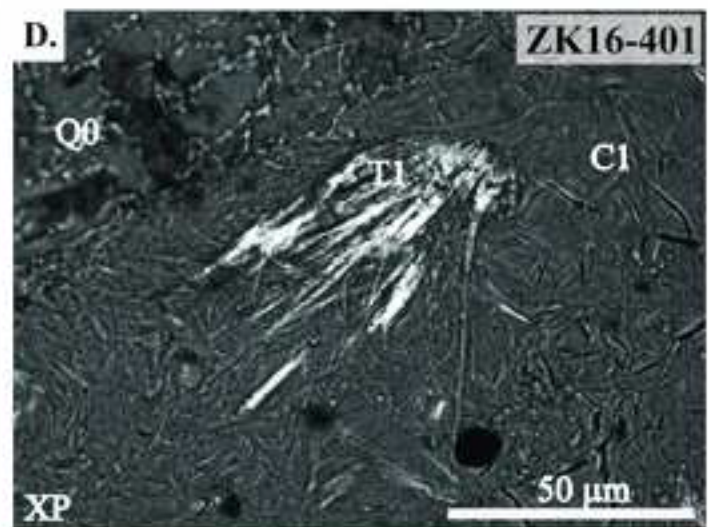
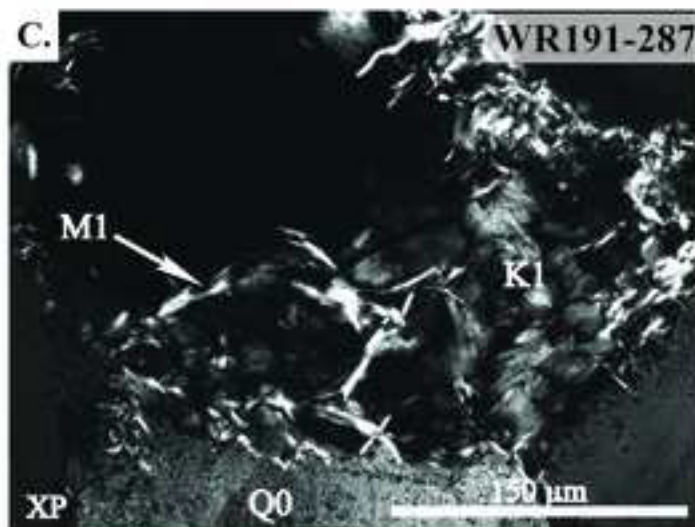
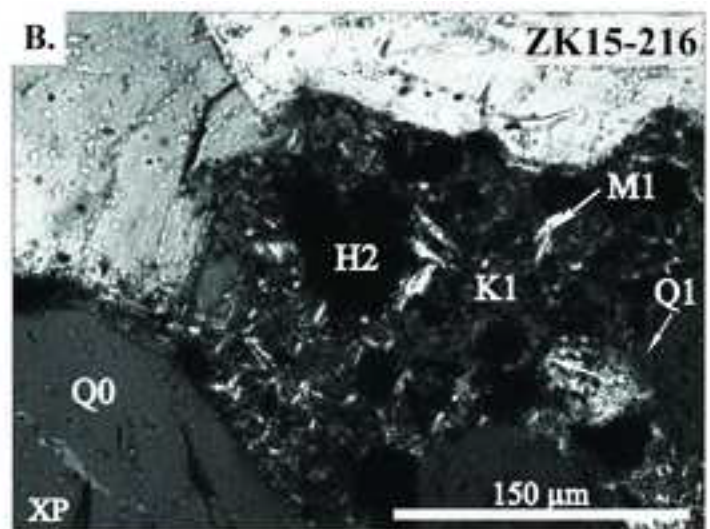
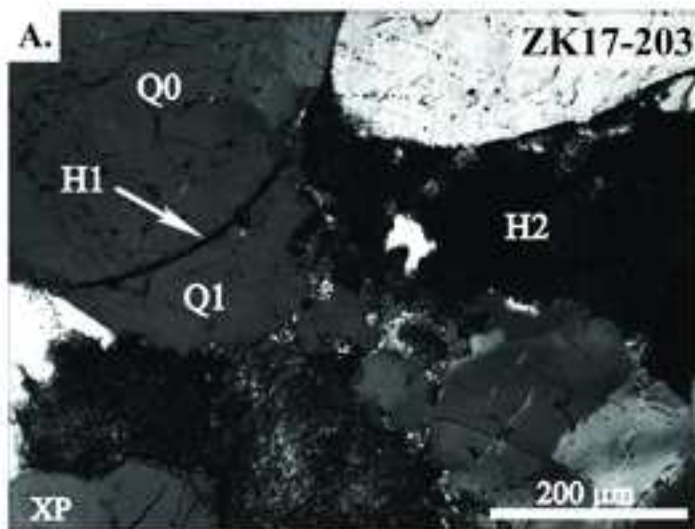


Figure 06

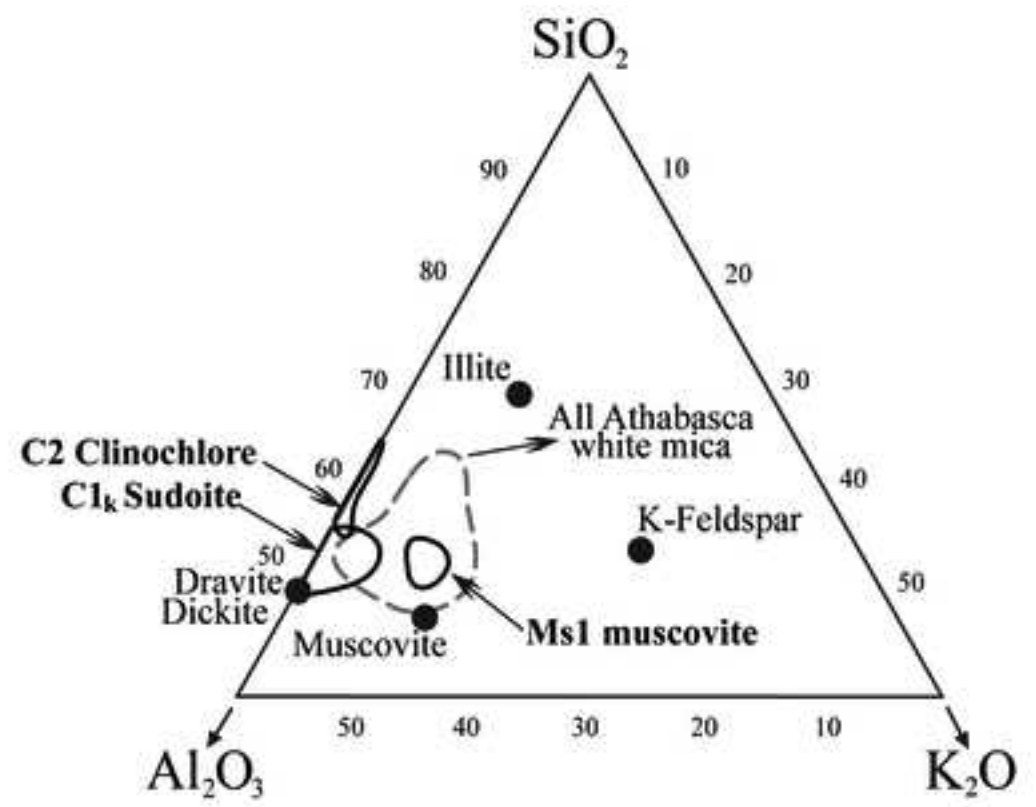
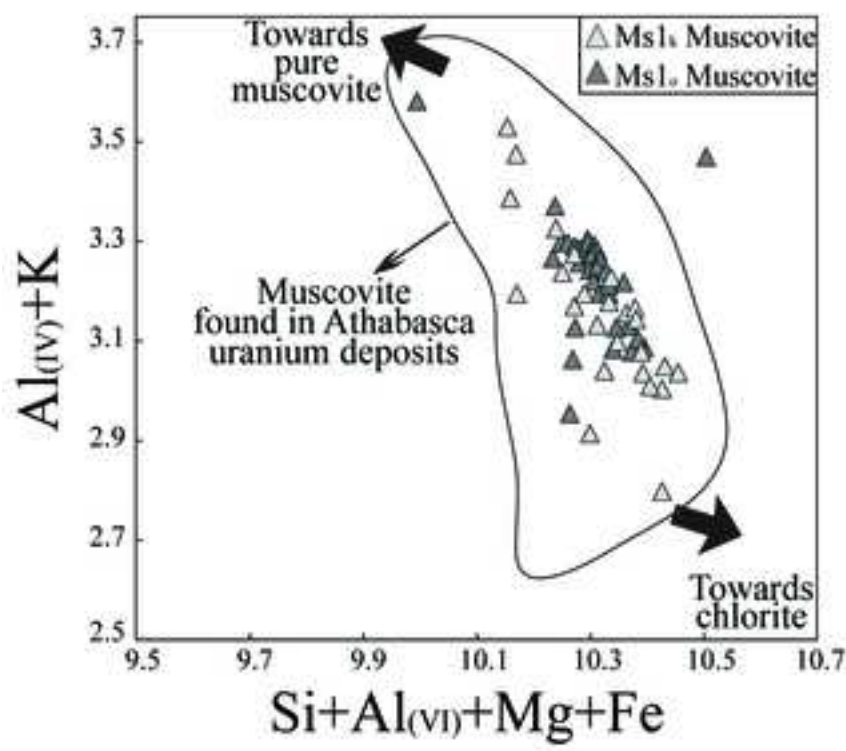


Figure 07

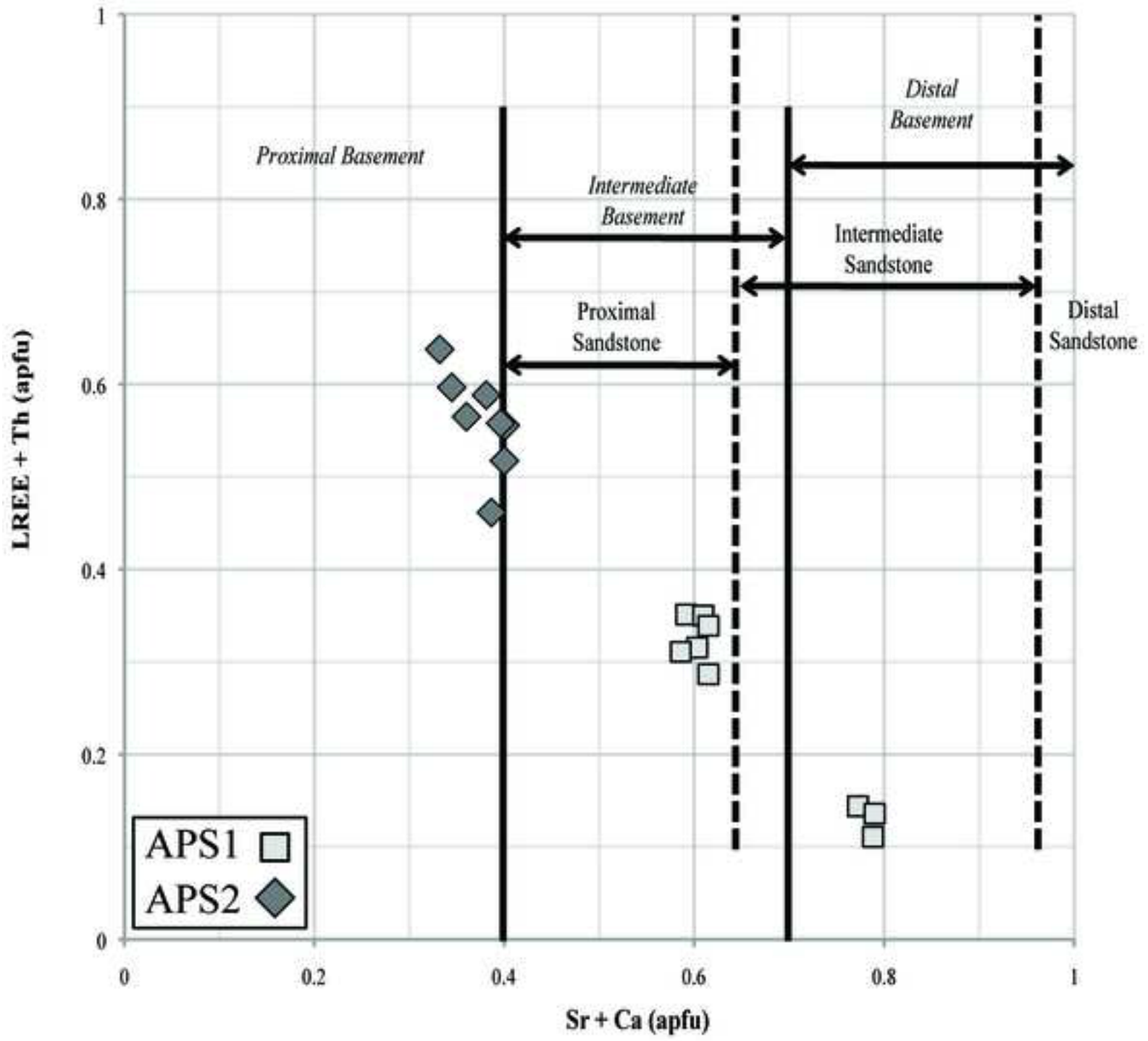


Figure 08

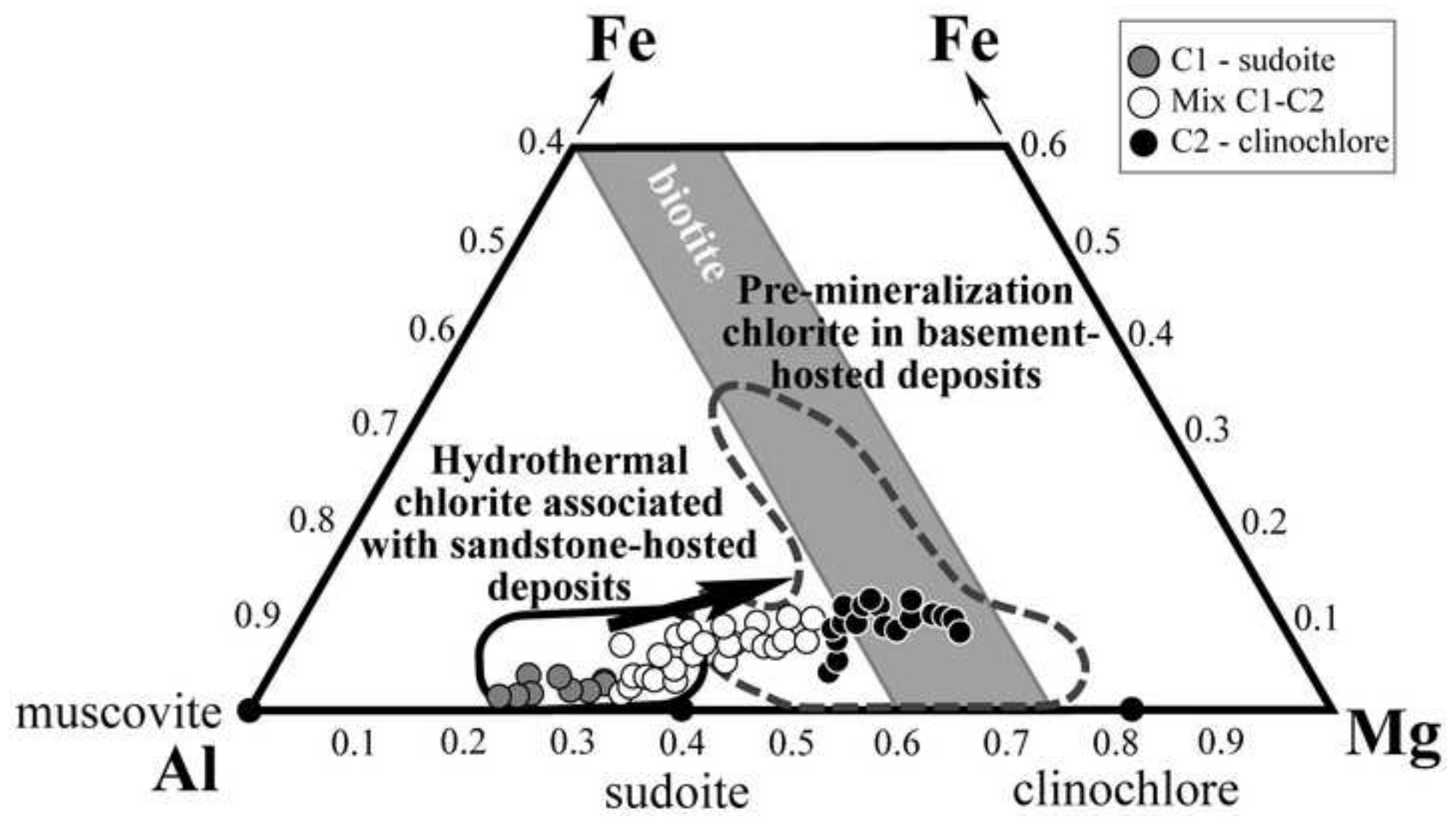


Figure 10

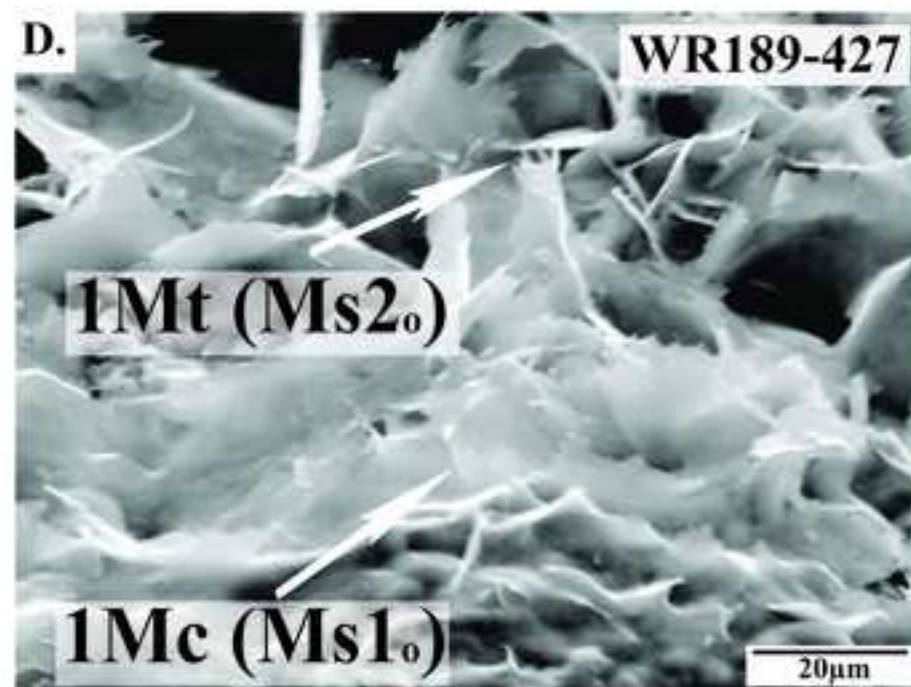
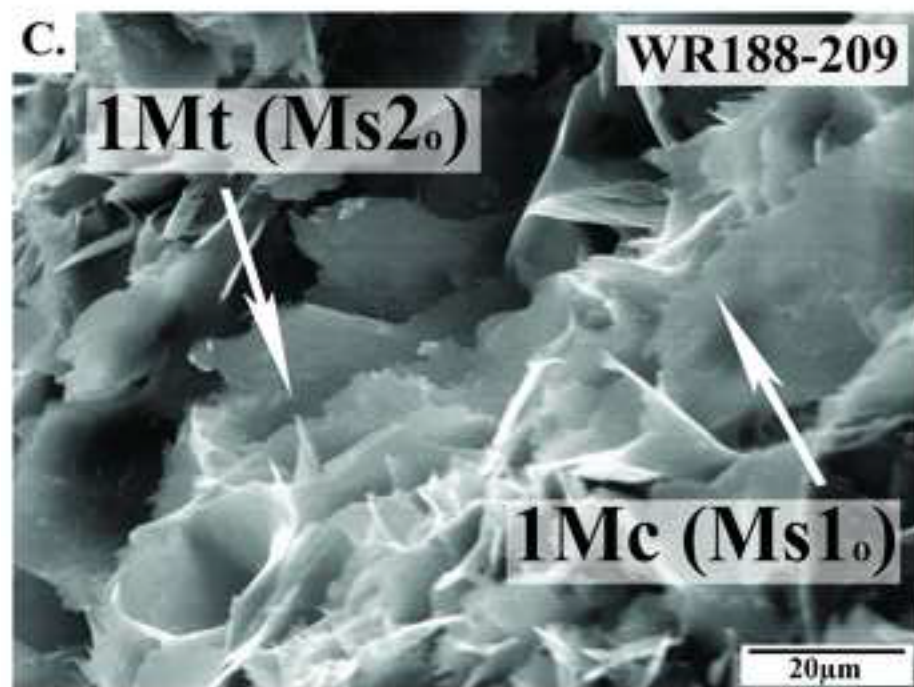
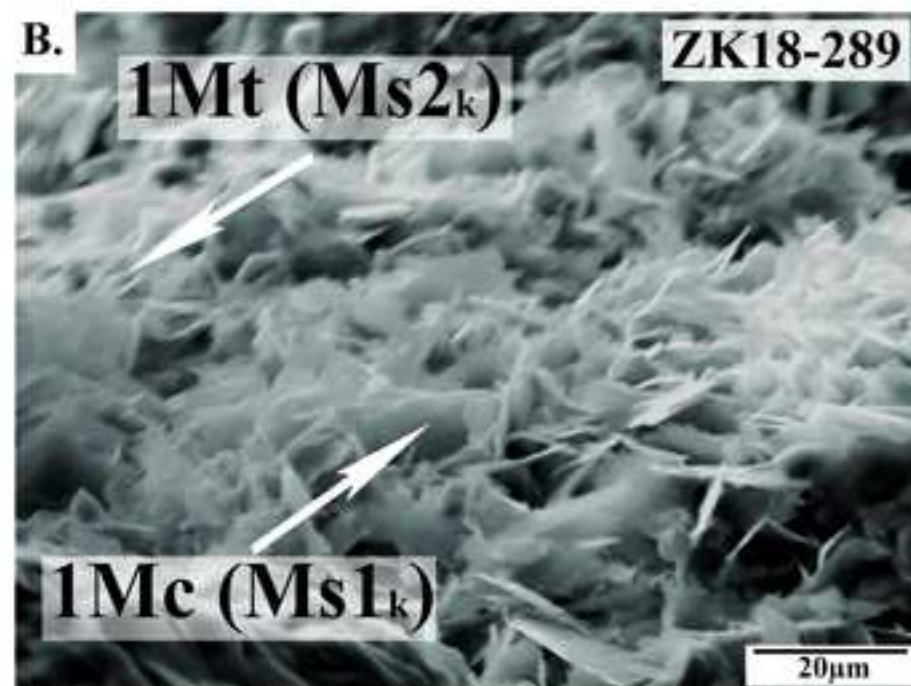
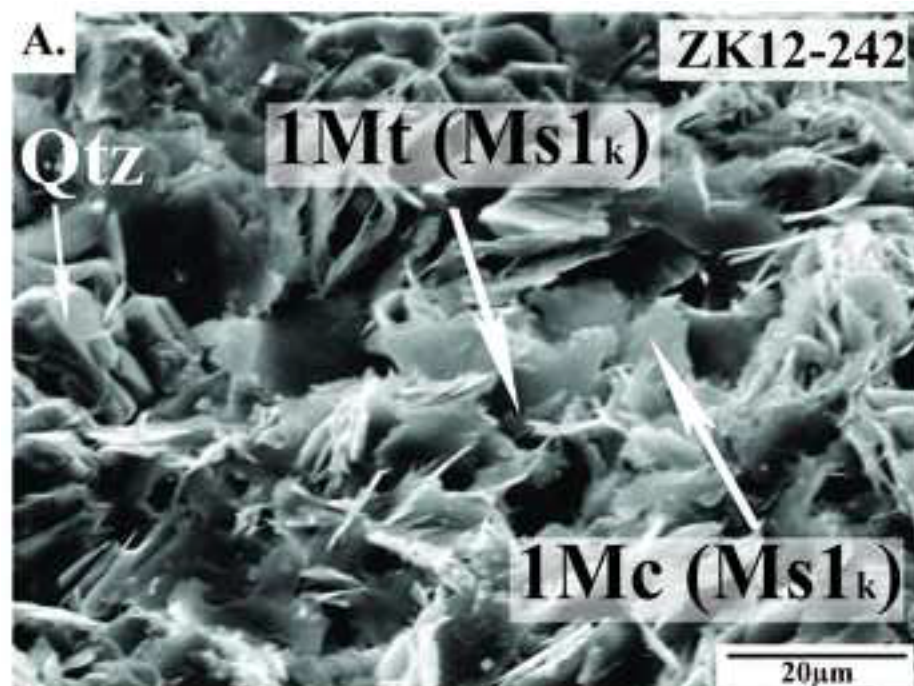


Figure 11

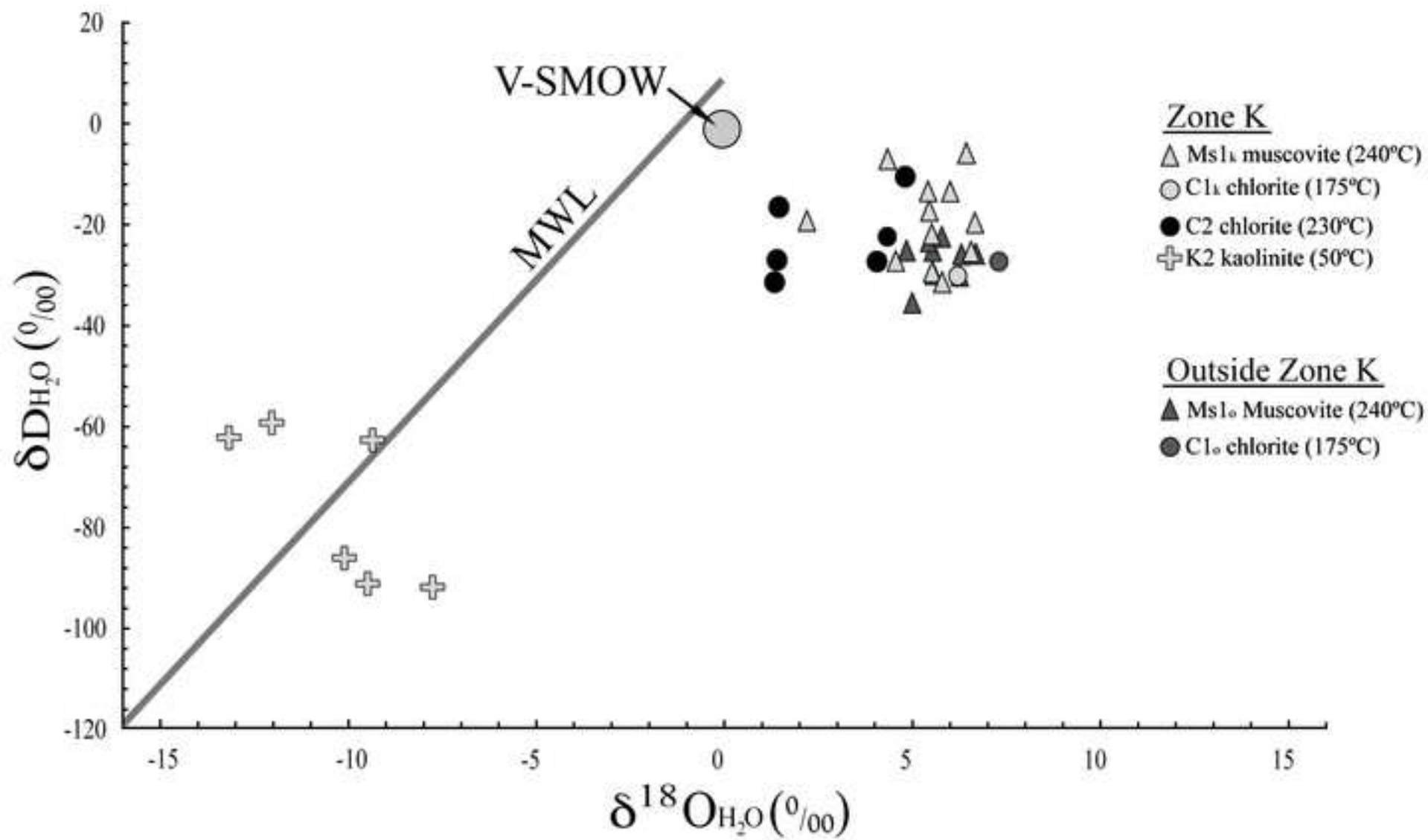


Figure 12

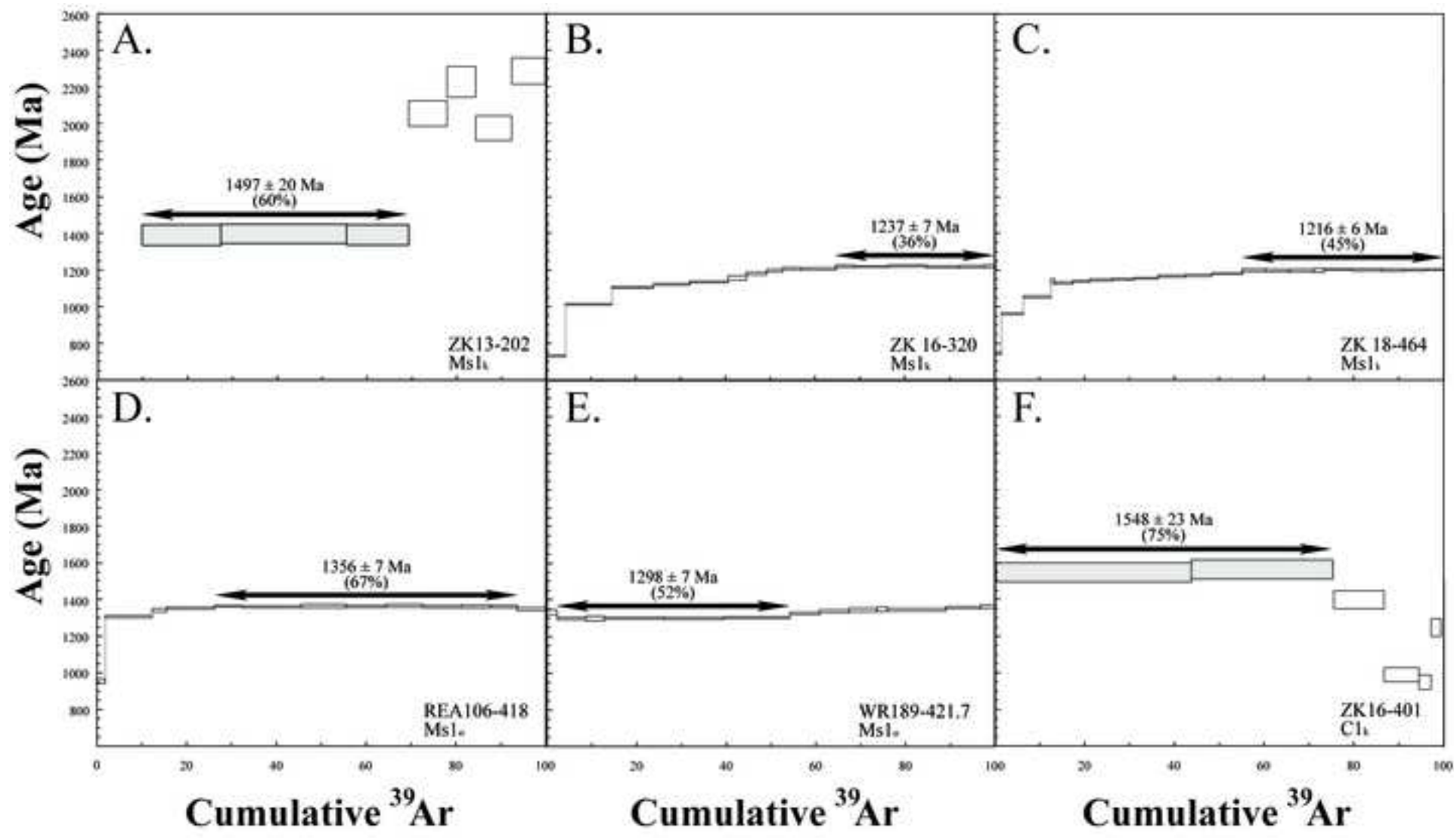


Figure 13

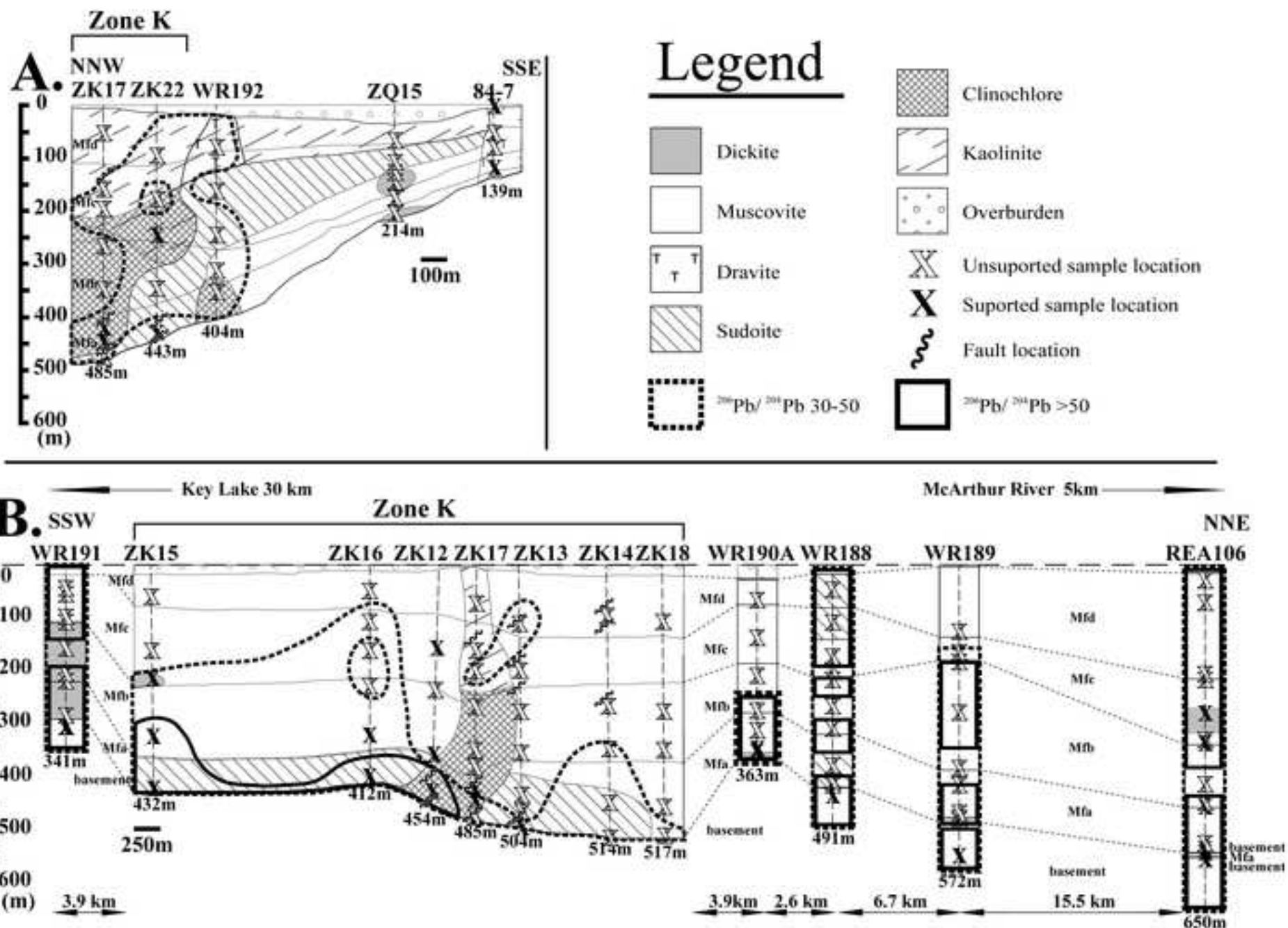


Figure 14

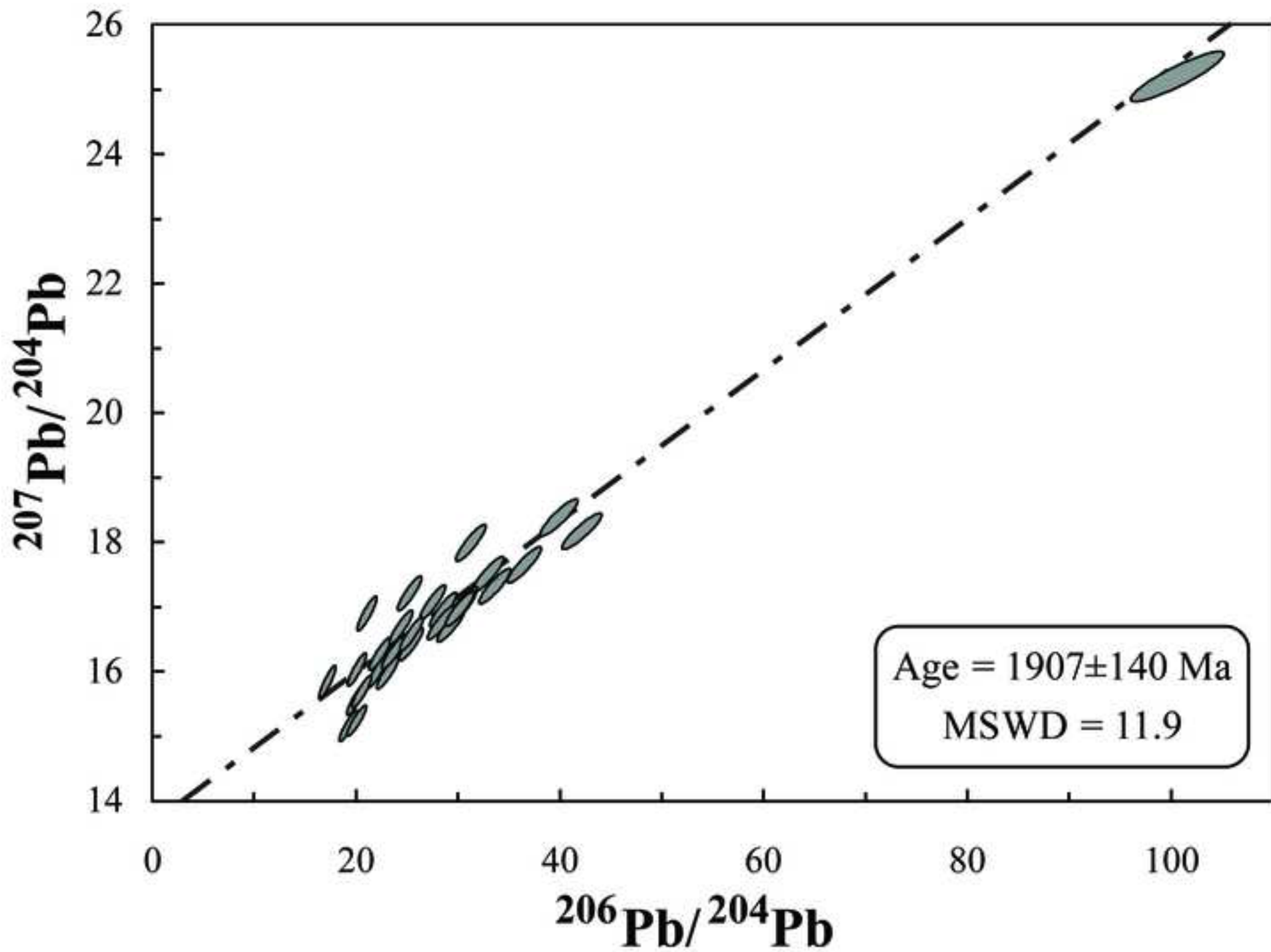
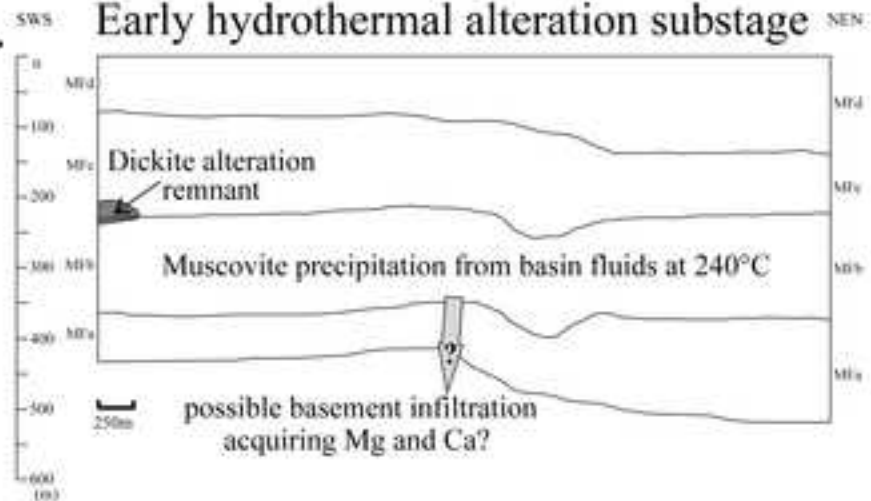
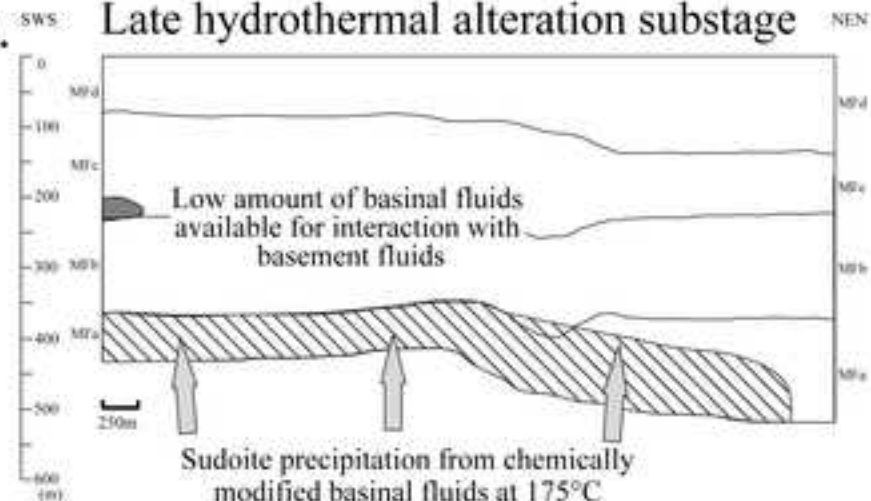


Figure 15

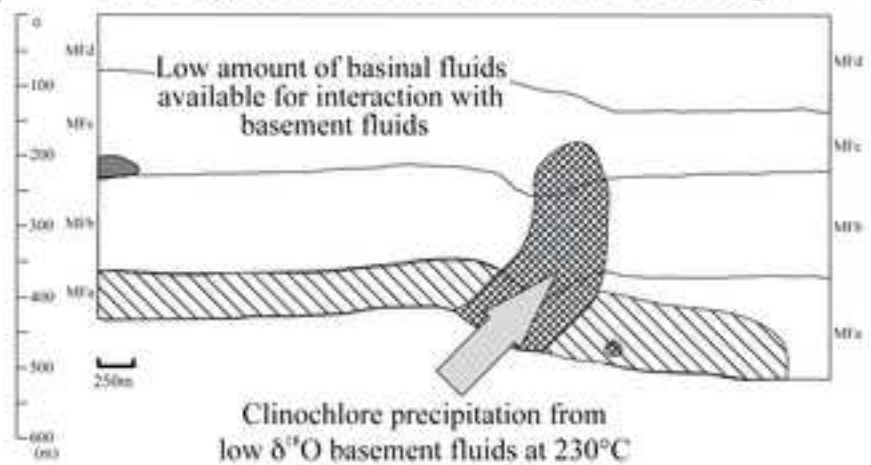
A. Early hydrothermal alteration substage



B. Late hydrothermal alteration substage



C. Late hydrothermal alteration substage



D. Post hydrothermal alteration stage

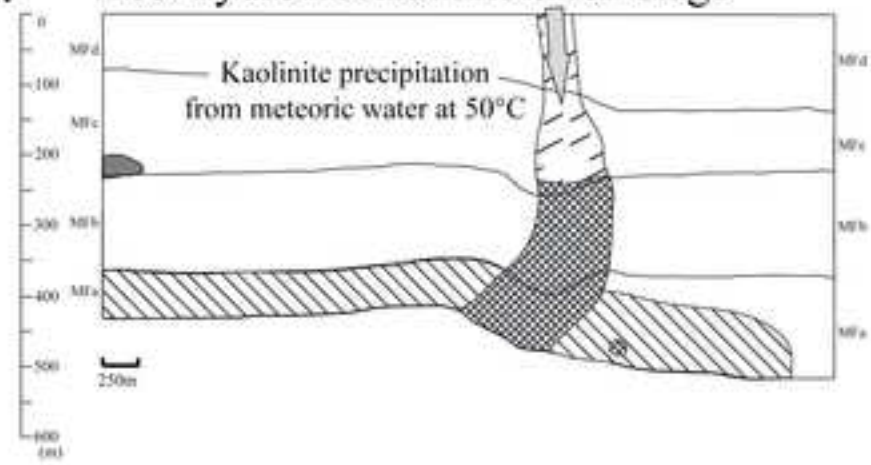


Table 1: Average Chemical Composition (in wt % and 1σ), Average Temperatures of Formation, and Average Structural Formulas of Various Muscovite and Chlorite Phases from the Wheeler River area.

	SiO ₂	TiO ₂	Al ₂ O ₃	Cr ₂ O ₃	FeO	MnO	MgO	CaO	Na ₂ O	K ₂ O	SUM	Temp. (°C)	Average half structural formula
Early hydrothermal alteration substage muscovite (Ms1 _k) (n=25)	48.1 ± 14	<DL	33.2 ± 1.2	<DL	1.2 ± 0.8	<DL	1.0 ± 0.3	0.1 ± 0.1	0.1 ± 0.1	9.3 ± 0.7	93.2 ± 1.6	240	K _{0.79} Mg _{0.10} Fe _{0.07} Al _{1.83} (Si _{3.23} Al _{0.77})O ₁₀ (OH) ₂
Early hydrothermal alteration substage muscovite (Ms1 _o) (n=31)	47.8 ± 1.1	<DL	33.7 ± 0.9	<DL	0.7 ± 0.2	<DL	0.7 ± 0.1	0.1 ± 0.1	<DL	9.5 ± 0.4	92.7 ± 1.8	240	K _{0.82} Mg _{0.07} Fe _{0.04} Al _{1.89} (Si _{3.22} Al _{0.78})O ₁₀ (OH) ₂
Mid hydrothermal alteration substage chlorite (C1 _k) (n=21)	33.5 ± 5.4	<DL	28.2 ± 5.0	<DL	1.4 ± 0.7	<DL	10.2 ± 3.3	0.1 ± 0.1	0.1 ± 0.1	1.1 ± 0.9	86.2 ± 3.3	175	Mg _{3.12} Fe _{0.23} Al _{5.95} (Si _{7.01} Al _{0.99})O ₂₀ (OH) ₁₆
Late hydrothermal alteration substage chlorite (C2) (n=22)	29.8 ± 2.5	<DL	19.2 ± 2.9	<DL	7.4 ± 1.1	<DL	21.8 ± 2.7	0.1 ± 0.1	<DL	0.1 ± 0.1	82.8 ± 3.4	230	Mg _{6.89} Fe _{1.31} Al _{3.07} (Si _{6.30} Al _{1.70})O ₂₀ (OH) ₁₆

Notes: Paragenesis of all phases analysed is shown in Figure 4; the variation of calculated temperatures is ± 30°C; see text for more discussion; n indicates the number of individual analyses on which the average was calculated; <DL = concentration lower than the detection limit.

Table 2: Chemical Composition (in wt % and 1) of Alumium Phosphate-Sulfate (APS) Phases from the Wheeler River Area.

	F	BaO	CaO	FeO	SrO	PbO ₂	ThO ₂	UO ₂	SO ₃	Al ₂ O ₃	La ₂ O ₃	Ce ₂ O ₃	Pr ₂ O ₃	Nd ₂ O ₃	V ₂ O ₃	P ₂ O ₅	Total
	(%)	(%)	(%)	(%)	(%)	(%)	(%)	(%)	(%)	(%)	(%)	(%)	(%)	(%)	(%)	(%)	(%)
Early hydrothermal alteration substage APS (APS1)																	
ZK12-242_01	0.72	0.61	2.82	1.99	13.55	0.18	0.81	<DL	6.38	34.64	1.08	2.40	0.25	0.81	<DL	23.78	94.47
ZK12-242_02	0.88	0.59	2.50	1.72	12.86	0.14	0.69	<DL	6.37	33.89	0.87	2.05	0.18	0.38	<DL	19.61	89.17
ZK12-242_03	1.09	0.59	2.75	1.89	11.93	<DL	0.84	<DL	5.66	31.82	1.04	2.44	0.23	0.97	<DL	21.17	88.85
ZK13-352_01	1.44	0.81	2.49	5.53	8.52	<DL	2.07	<DL	3.87	30.19	2.47	5.32	0.43	1.54	<DL	19.67	84.93
ZK13-352_02	1.17	0.66	2.50	3.69	7.90	0.15	1.83	<DL	3.49	28.49	2.70	5.37	0.54	1.42	<DL	19.58	81.28
ZK13-352_03	1.37	0.72	2.26	2.80	8.14	0.20	2.12	<DL	4.44	29.39	2.57	5.61	0.53	1.62	<DL	19.49	81.90
ZK13-352_04	1.14	1.14	2.62	3.87	8.69	0.16	2.21	<DL	3.55	30.82	2.42	5.94	0.58	1.63	<DL	21.49	86.86
ZK13-352_05	1.17	1.40	2.34	4.05	8.21	<DL	1.96	<DL	4.21	29.70	2.14	5.64	0.68	1.20	<DL	21.30	84.54
ZK13-352_06	1.24	1.20	2.41	3.37	9.06	0.20	2.00	<DL	4.91	30.64	2.16	4.97	0.19	1.59	<DL	21.25	85.77
average:	1.14	0.86	2.52	3.21	9.87	0.13	1.61	<DL	4.77	31.07	1.94	4.41	0.40	1.24	<DL	20.81	86.42
Late hydrothermal alteration substage APS (APS2)																	
ZK22-262-01	0.97	0.24	2.08	5.76	4.54	<DL	0.46	<DL	2.72	30.05	4.43	9.07	0.79	2.86	<DL	19.72	87.52
ZK22-262-02	0.87	0.18	1.88	4.47	4.11	<DL	0.40	<DL	2.38	29.84	4.68	9.84	0.89	3.22	<DL	21.68	87.68
ZK22-262-03	0.96	0.30	2.16	2.77	3.79	<DL	0.33	0.10	2.31	28.39	4.79	10.25	0.60	3.34	<DL	22.32	84.77
ZK22-262-04	0.78	0.19	1.71	0.97	4.17	<DL	0.38	<DL	2.81	27.41	4.09	8.65	0.81	2.80	<DL	19.90	78.86
ZK22-262-05	0.92	0.22	2.05	1.85	4.37	<DL	0.46	<DL	2.53	30.17	4.49	9.17	0.90	3.15	<DL	20.74	87.07
ZK22-262-07	0.61	0.17	1.54	1.61	3.49	<DL	0.19	<DL	2.60	25.69	3.03	6.40	0.72	1.75	<DL	15.73	73.04
ZK22-262-08	0.94	0.12	1.54	0.92	4.56	<DL	0.28	<DL	2.90	31.13	5.01	10.58	1.14	3.47	<DL	24.16	88.01
ZK22-262-09	0.84	0.21	1.56	1.33	3.91	<DL	0.28	0.14	2.48	28.79	4.94	10.99	1.09	3.57	<DL	23.40	85.53
average:	0.86	0.20	1.81	2.46	4.12	<DL	0.35	0.07	2.59	28.93	4.43	9.37	0.87	3.02	<DL	20.96	84.06

Notes: Paragenesis of all phases analysed is shown in Figure 4; see text for more discussion; <DL = concentration lower than the detection limit. APS compositions have been corrected for their muscovite and chlorite content.

Table 3. Measured Mineral $\delta^{18}\text{O}$ and δD and Calculated $\delta^{18}\text{O}$ and δD Values for Fluids in Equilibrium with Alteration Clay-sized Minerals from the Wheeler River Area.

Sample	fraction size	Mineral		Water	
		δD	$\delta^{18}\text{O}$	δD	$\delta^{18}\text{O}$
<u>Early hydrothermal alteration Muscovite (Ms_{1c}) from the Zone K</u>					
ZK12-160	<2	-50	7.3	-20	2.1
ZK12-242	<2	-37	11.6	-7	6.4
ZK12-360	<2	-38	9.4	-8	4.3
ZK13-279	<2	-56	11.8	-26	6.7
ZK13-279	2-5	-44	11.2	-14	6.0
ZK13-352	<2	-48	10.6	-18	5.4
ZK14-100	<2	-62	11.0	-32	5.9
ZK15-325	<2	-53	10.7	-23	5.5
ZK16-320	<2	-58	9.8	-28	4.6
ZK18-289	<2	-60	10.8	-30	5.6
ZK18-351	<2	-44	10.5	-14	5.3
ZK18-464	<2	-50	12.0	-20	6.8
<u>Early hydrothermal alteration Muscovite (Ms_{1o}) from outside the Zone K</u>					
REA106-333	<2	-61	10.7	-31	5.6
REA106-418	<2	-66	10.1	-36	5.0
WR188-175	<2	-55	10.9	-25	5.7
WR188-209	<2	-55	10.1	-25	4.9
WR188-310	<2	-53	11.1	-23	5.9
WR189-421.7	<2	-57	12.0	-27	6.8
WR190A-321	<2	-52	10.5	-22	5.3
WR191-045	2-5	-61	11.3	-31	6.1
WR191-060.5	<2	-57	11.3	-27	6.1
<u>Mid hydrothermal alteration Chlorite (Cl_{1c}) from the Zone K</u>					
ZK15-425	<2	-59	10.4	-27	7.3
<u>Mid hydrothermal alteration Chlorite (Cl_{1o}) from outside the Zone K</u>					
WR188-380	<2	-62	9.3	-30	6.2
<u>Late hydrothermal alteration Chlorite (C2)</u>					
ZK12-430	<2	-37	6.3	-10	4.8
ZK17-270	<2	-58	2.8	-31	1.4
ZK17-381	<2	-54	5.6	-27	4.1
ZK17-426	<2	-43	3.0	-16	1.5
ZK17-446	<2	-54	2.9	-27	1.4
ZK13-480	<2	-46	3.0	-19	1.6
<u>Late alteration Kaolinite (K2)</u>					
ZK17-077	<2	-120	11.9	-92	-7.8
ZK17-163	<2	-115	9.6	-86	-10.1
ZK17-163	2-5	-120	10.3	-91	-9.4
ZK17-203	<2	-91	6.6	-62	-13.1
ZK22-99	<2	-90	10.4	-62	-9.3
ZK22-262	<2	-88	7.7	-59	-12.0

Notes: The temperatures used to calculate the fluid values are derived from the crystal chemistry of the clay minerals; the variation of the individual O and H analyses are ± 0.2 and ± 3 per mil; see the text for more details

Table 4. Result of the $^{40}\text{Ar}/^{39}\text{Ar}$ dating of Ms1_k and Ms1_o muscovites and C1_k chlorite from the Wheeler River area

Sample	Mineral	Location	Plateau or pseudo-plateau age (Ma)	Length of plateau (% of gas released)	Oldest step age (Ma)
ZK13-202	Muscovite	Zone K	1497 ± 20	60.1	2391 ± 72
ZK16-320	Muscovite	Zone K	1237 ± 7	35.6	1240 ± 5
ZK18-464	Muscovite	Zone K	1216 ± 6	44.9	1218 ± 4
REA106-418	Muscovite	Outside Zone K	1356 ± 7	67.4	1360 ± 8
WR189-421.7	Muscovite	Outside Zone K	1298 ± 7	51.7	1360 ± 9
ZK16-401	Chlorite	Zone K	1548 ± 23	75.2	1558 ± 52

Appendix I. Pb isotopic compositions and concentrations of several elements in the leachates from the Manitou Falls Formation at Wheeler River.

Sample	Source of Pb	$^{206}\text{Pb}/^{204}\text{Pb}$	$^{207}\text{Pb}/^{204}\text{Pb}$	$^{207}\text{Pb}/^{206}\text{Pb}$	$^{207}\text{Pb}/^{206}\text{Pb}$ age	$^{207}\text{Pb}/^{235}\text{U}$	$^{206}\text{Pb}/^{238}\text{U}$	Ca (ppb)	Co (ppb)	Cu (ppb)	Ni (ppb)	P (ppb)	Pb (ppb)	Sr (ppb)	Th (ppb)	U (ppb)	Zn (ppb)	Zr (ppb)
Zone K Trend:																		
ZK12-160	Supported	24	16	0.65	4613	46.65	0.51	11.05	0.08	0.85	0.13	0.84	0.11	0.33	0.07	0.06	0.11	0.52
ZK12-242	Unsupported	19	15	0.79	4901	190.25	1.65	50.90	0.08	0.63	0.10	1.99	0.12	0.67	0.04	0.02	1.57	0.45
ZK12-360	Supported	25	13	0.52	4310	43.37	0.57	55.36	0.16	1.35	0.11	<DL	0.22	0.79	0.96	0.06	1.37	0.81
ZK12-430	Supported	56	19	0.34	3656	6.95	0.14	2035	0.61	4.00	0.75	1484	0.20	5.04	0.65	0.90	0.49	1.69
ZK13-117	Unsupported	33	18	0.53	4333	7746.50	102.94	16.24	0.17	2.44	0.46	0.61	6.73	0.25	<DL	0.02	0.87	0.26
ZK13-202	Unsupported	20	15	0.76	4849	154.62	2.12	10.51	0.02	2.12	0.03	<DL	0.14	0.21	<DL	0.02	0.11	0.19
ZK13-279	Unsupported	20	16	0.78	4883	193.69	1.72	7.20	0.04	1.98	0.07	<DL	0.09	0.21	<DL	0.02	0.22	0.16
ZK13-352	Unsupported	24	16	0.67	4676	543.17	5.63	26.07	0.16	3.15	0.19	0.95	0.82	0.71	0.13	0.04	0.63	0.33
ZK13-440	Unsupported	25	17	0.66	4648	135.04	1.44	21.42	0.08	1.14	0.20	2.29	0.23	0.33	0.03	0.06	0.73	0.42
ZK13-480	Unsupported	21	16	0.76	4852	125.05	1.21	17.89	0.11	1.57	0.14	1.10	0.15	0.41	0.11	0.04	0.66	0.16
ZK14-100	Unsupported	29	17	0.57	4437	646.94	7.75	10.03	0.04	2.42	0.11	<DL	0.54	0.28	<DL	0.03	0.22	0.23
ZK14-264	Unsupported	22	16	0.72	4781	823.40	7.76	19.24	0.07	2.42	0.14	0.53	0.21	0.41	<DL	0.01	0.19	0.20
ZK14-350	Unsupported	34	17	0.52	4290	72.36	0.98	93.37	0.78	2.42	2.57	1.97	0.21	1.39	0.59	0.05	0.32	0.27
ZK14-453	Unsupported	101	25	0.25	3188	14.71	0.41	17.88	1.37	6.49	3.78	2.54	0.18	0.64	1.05	0.19	5.84	0.57
ZK14-514	Unsupported	30	17	0.56	4416	43.91	0.51	30.05	2.33	5.18	3.52	0.85	4.67	1.00	0.61	3.02	0.55	0.56
ZK15-064	Unsupported	25	17	0.68	4691	65.34	1.21	12.77	0.02	4.20	0.12	<DL	0.18	0.29	<DL	0.05	0.82	0.15
ZK15-163	Unsupported	23	16	0.69	4715	336.54	3.28	82.02	0.08	2.63	0.10	<DL	0.16	0.47	0.09	0.02	0.15	0.11
ZK15-216	Supported	34	18	0.52	4294	33.21	0.45	21.72	0.10	0.85	0.75	<DL	0.08	0.44	0.03	0.06	<DL	0.09
ZK15-325	Supported	52	19	0.36	3768	14.71	0.28	733.7	0.06	1.96	0.05	361.9	0.26	3.70	0.44	0.60	0.20	0.93
ZK15-425	Supported	89	22	0.25	3189	5.01	0.13	1373	0.27	3.66	0.76	308.6	0.28	4.83	0.79	1.86	0.39	0.66
ZK16-049	Unsupported	20	16	0.80	4917	241.10	3.55	9.03	0.03	1.00	0.04	0.20	0.18	0.26	0.02	0.02	0.05	0.24
ZK16-110	Unsupported	31	17	0.56	4409	380.62	4.54	8.24	0.03	4.71	0.09	<DL	0.25	0.20	<DL	0.02	0.47	0.23
ZK16-169	Unsupported	26	17	0.65	4631	70.46	0.75	15.57	0.26	0.56	2.02	<DL	0.23	0.41	0.08	0.10	0.45	0.23

Appendix I (continued). Pb isotopic compositions and concentrations of several elements in the leachates from the Manitou Falls Formation at Wheeler River.

Sample	Source of Pb	$^{206}\text{Pb}/^{204}\text{Pb}$	$^{207}\text{Pb}/^{204}\text{Pb}$	$^{207}\text{Pb}/^{206}\text{Pb}$	$^{207}\text{Pb}/^{206}\text{Pb}$ age	$^{207}\text{Pb}/^{235}\text{U}$	$^{206}\text{Pb}/^{238}\text{U}$	Ca (ppb)	Co (ppb)	Cu (ppb)	Ni (ppb)	P (ppb)	Pb (ppb)	Sr (ppb)	Th (ppb)	U (ppb)	Zn (ppb)	Zr (ppb)
ZK16-235	Unsupported	29	16	0.55	4376	65.69	0.80	36.66	0.08	0.61	0.14	<DL	0.07	0.30	0.05	0.03	0.07	0.13
ZK16-320	Supported	32	18	0.55	4377	18.52	0.24	130.4	0.06	0.65	0.08	1.99	0.25	1.63	14.60	0.14	0.14	0.20
ZK16-401	Supported	105	24	0.22	3007	0.58	0.02	19.93	0.21	5.14	1.12	0.87	0.04	0.46	0.11	0.88	0.36	0.11
ZK17-077	Unsupported	23	16	0.73	4788	705.79	7.58	7.20	0.12	1.30	0.18	<DL	0.26	0.17	<DL	<DL	0.12	0.21
ZK17-163	Unsupported	24	16	0.69	4708	150.47	1.52	9.21	0.33	2.92	0.81	0.90	0.19	0.23	0.02	0.04	1.03	0.15
ZK17-203	Unsupported	31	17	0.56	4407	110.70	1.44	98.30	1.13	198.2	1.38	0.73	0.32	0.73	0.16	0.13	0.84	1.07
ZK17-270	Unsupported	29	17	0.59	4494	74.95	0.90	57.98	0.42	93.21	1.04	3.23	0.32	0.95	0.20	0.17	1.02	0.52
ZK17-354	Unsupported	17	16	0.92	5121	682.47	6.47	39.14	0.34	92.46	0.25	<DL	0.87	0.70	0.25	0.09	0.44	0.44
ZK17-426	Supported	27	17	0.63	4568	15.26	0.17	54.62	0.47	3.99	0.93	<DL	0.73	1.14	0.84	0.43	1.64	0.75
ZK17-446	Supported	31	17	0.54	4368	29.26	0.37	28.05	0.24	33.02	0.41	7.25	0.35	0.73	0.13	0.38	0.57	0.31
ZK17-483	Unsupported	42	18	0.43	4025	32.85	0.49	107.3	0.56	7.93	1.03	3.68	4.42	2.93	0.15	3.91	0.32	0.23
ZK18-112	Unsupported	21	17	0.80	4924	564.55	4.78	17.23	0.02	13.13	0.06	<DL	0.08	0.25	0.01	<DL	0.08	0.19
ZK18-289	Unsupported	26	17	0.65	4618	355.83	3.89	73.42	0.04	4.67	0.09	12.00	1.40	1.89	0.36	0.10	0.51	0.43
ZK18-351	Unsupported	29	17	0.59	4488	223.74	4.71	20.27	0.04	14.99	0.09	3.63	0.63	1.85	0.78	0.04	0.28	0.59
ZK18-464	Unsupported	28	17	0.62	4558	100.26	1.13	70.32	0.05	7.65	0.19	12.26	0.13	1.44	0.03	0.04	0.38	0.54
ZK18-517	Unsupported	31	18	0.58	4447	86.61	3.28	41.35	<DL	3.42	0.06	3.12	0.29	0.52	0.14	0.02	0.17	0.26
ZK22-099	Unsupported	37	18	0.48	4194	135.63	2.07	6.60	3.99	6.39	7.91	16.82	0.15	0.24	0.03	0.05	1.15	0.42
ZK22-189	Unsupported	25	17	0.68	4697	125.80	1.30	23.41	0.42	47.42	1.25	0.90	0.17	0.47	0.35	0.05	0.72	0.64
ZK22-262	Supported	37	19	0.51	4262	22.96	0.30	17.68	6.95	185.5	6.70	<DL	0.08	0.26	0.04	0.11	0.82	0.45
ZK22-349	Unsupported	40	18	0.46	4123	112.07	1.78	40.98	0.27	2.53	0.37	<DL	0.29	0.59	0.11	0.06	0.20	0.14
ZK22-436	Supported	29	17	0.59	4472	37.86	0.45	85.17	0.32	49.10	0.53	1.35	0.67	1.94	0.19	0.55	2.60	0.18
Outside Zone K Trend:																		
84-7-015	Supported	25	17	0.68	4680	55.58	0.56	8.57	0.01	1.88	0.06	<DL	0.08	0.29	0.02	0.06	0.20	0.29
84-7-059	Unsupported	22	16	0.76	4841	108.01	1.01	12.18	0.02	0.68	0.07	0.80	0.16	0.43	0.03	0.06	0.96	0.52

Appendix I (continued). Pb isotopic compositions and concentrations of several elements in the leachates from the Manitou Falls Formation at Wheeler River.

Sample	Source of Pb	²⁰⁶ Pb/ ²⁰⁴ Pb	²⁰⁷ Pb/ ²⁰⁴ Pb	²⁰⁷ Pb/ ²⁰⁶ Pb	²⁰⁷ Pb/ ²⁰⁶ Pb age	²⁰⁷ Pb/ ²³⁵ U	²⁰⁶ Pb/ ²³⁸ U	Ca (ppb)	Co (ppb)	Cu (ppb)	Ni (ppb)	P (ppb)	Pb (ppb)	Sr (ppb)	Th (ppb)	U (ppb)	Zn (ppb)	Zr (ppb)
WR188-434	Supported	100	30	0.30	3484	2.55	0.06	534.4	0.02	1.58	0.28	257.7	0.19	9.67	0.03	1.97	0.20	0.12
WR189-131	Unsupported	25	21	0.86	5027	847.97	8.12	3.03	0.05	6.55	<DL	0.65	0.31	0.30	0.03	0.02	0.83	0.14
WR189-169.5	Unsupported	38	32	0.84	4997	193.25	5.02	5.43	<DL	2.61	<DL	1.05	0.19	0.41	0.02	<DL	2.22	0.09
WR189-189.6	Unsupported	2883	1620	0.56	4412	53.12	0.69	4.85	0.03	3.27	<DL	0.74	0.15	0.43	0.11	0.07	0.97	0.09
WR189-289.5	Unsupported	118	92	0.78	4889	171.55	1.77	44.96	<DL	2.03	<DL	0.43	0.12	0.86	0.08	0.02	3.03	0.12
WR189-389.4	Unsupported	21	16	0.78	4882	66.38	7.18	22.51	0.03	3.74	0.04	0.54	0.21	0.67	0.03	0.01	1.41	0.07
WR189-421.7	Unsupported	275	222	0.81	4936	235.23	2.32	12.45	0.11	5.86	0.08	0.81	0.15	0.84	0.02	0.02	1.86	0.16
WR189-472.3	Unsupported	²⁰⁴ Pb <DL	²⁰⁴ Pb <DL	0.73	4791	171.34	2.05	16.29	<DL	2.44	0.07	<DL	0.08	0.99	0.05	<DL	2.30	0.26
WR189-484	Unsupported	35	24	0.69	4711	26.06	1.03	20.86	0.05	3.10	0.07	<DL	0.21	1.29	0.21	0.04	1.68	0.30
WR189-486	Unsupported	51	26	0.51	4266	107.65	1.54	30.22	<DL	1.89	0.06	<DL	0.41	2.06	0.06	0.08	1.48	0.12
WR189-557	Supported	²⁰⁴ Pb <DL	²⁰⁴ Pb <DL	0.35	3703	9.85	0.19	1249	0.03	1.38	0.05	496.1	0.14	11.81	0.30	0.36	2.76	0.58
WR190A-074.3	Unsupported	26	22	0.86	5018	130.37	2.20	16.18	0.06	6.64	0.08	0.93	0.33	0.52	0.04	0.05	2.89	0.13
WR190A-144.5	Unsupported	23	19	0.83	4967	38.79	1.00	21.13	0.06	2.95	0.09	0.66	0.14	0.47	0.05	0.04	0.73	0.10
WR190A-222.3	Unsupported	23	18	0.77	4859	29.37	2.01	13.86	0.02	2.05	<DL	<DL	0.08	0.57	<DL	<DL	1.48	<DL
WR190A-294	Unsupported	55	40	0.74	4813	194.41	2.02	48.58	0.02	2.15	0.03	2.32	0.23	0.73	0.50	0.02	0.18	0.08
WR190A-321	Unsupported	²⁰⁴ Pb <DL	²⁰⁴ Pb <DL	0.76	4856	80.00	0.72	20.04	0.02	2.00	0.07	0.82	0.06	0.92	0.02	0.02	1.18	0.08
WR190A-352.3	Supported	83	46	0.55	4392	14.34	0.18	22.35	0.02	8.87	0.18	0.69	0.13	1.03	<DL	0.30	2.13	0.09
WR190A-362.3	Supported	²⁰⁴ Pb <DL	²⁰⁴ Pb <DL	0.69	4717	25.25	0.25	6.86	0.02	2.45	0.06	0.78	0.09	0.40	<DL	0.12	1.43	0.12
WR191-045	Unsupported	65	52	0.80	4929	324.20	3.16	9.48	<DL	12.11	0.08	<DL	0.17	0.24	<DL	0.02	1.22	<DL
WR191-060-5	Unsupported	77	65	0.83	4982	81.92	1.93	13.10	<DL	2.38	0.04	0.68	0.10	0.30	<DL	0.02	0.42	<DL
WR191-100	Unsupported	²⁰⁴ Pb <DL	²⁰⁴ Pb <DL	0.81	4939	132.12	1.32	7.75	<DL	2.93	<DL	1.02	0.07	0.32	<DL	0.02	1.92	<DL
WR191-110	Unsupported	19	17	0.90	5097	1694.32	15.01	13.71	0.07	3.06	0.06	1.87	0.92	0.39	0.03	0.02	3.31	<DL
WR191-160	Unsupported	79	54	0.69	4709	51.03	0.65	27.80	0.04	2.61	0.07	0.78	0.35	0.92	1.53	0.08	2.70	0.09
WR191-207.6	Unsupported	136	109	0.80	4924	192.57	1.91	17.66	0.08	2.70	0.14	<DL	0.22	0.40	0.09	0.03	2.93	0.13
WR191-220	Unsupported	²⁰⁴ Pb <DL	²⁰⁴ Pb <DL	0.79	4900	42.67	2.24	12.62	<DL	2.87	0.10	0.68	0.07	0.33	<DL	0.01	1.34	0.06
WR191-287	Unsupported	²⁰⁴ Pb <DL	²⁰⁴ Pb <DL	0.47	4143	32.06	0.47	13.20	0.06	1.82	0.13	0.66	0.10	0.50	0.04	0.11	0.67	0.13

Appendix I (end). Pb isotopic compositions and concentrations of several elements in the leachates from the Manitou Falls Formation at Wheeler River.

Sample	Source of Pb	$^{206}\text{Pb}/^{204}\text{Pb}$	$^{207}\text{Pb}/^{204}\text{Pb}$	$^{207}\text{Pb}/^{206}\text{Pb}$	$^{207}\text{Pb}/^{206}\text{Pb}$ age	$^{207}\text{Pb}/^{235}\text{U}$	$^{206}\text{Pb}/^{238}\text{U}$	Ca (ppb)	Co (ppb)	Cu (ppb)	Ni (ppb)	P (ppb)	Pb (ppb)	Sr (ppb)	Th (ppb)	U (ppb)	Zn (ppb)	Zr (ppb)
WR191-306.5	Supported	$^{204}\text{Pb} < \text{DL}$	$^{204}\text{Pb} < \text{DL}$	0.25	3209	3.27	0.09	856.5	0.06	0.96	0.25	509.8	0.15	36.25	0.38	1.10	1.46	0.14
WR192-080	Unsupported	49	22	0.45	4087	200.06	3.20	6.54	0.15	19.47	0.35	<DL	0.09	0.32	0.04	0.04	0.17	0.47
WR192-167	Unsupported	23	17	0.72	4779	166.31	1.66	12.83	0.06	1.41	0.11	<DL	0.21	0.40	0.04	0.06	0.49	0.22
WR192-251	Unsupported	44	19	0.43	4025	36.60	0.60	71.53	1.18	2.69	2.86	4.60	0.36	5.70	6.06	0.18	0.21	0.29
WR192-318	Unsupported	38	18	0.47	4155	80.90	1.16	35.88	0.06	14.51	0.20	<DL	0.17	0.61	0.09	0.04	0.06	0.18
WR192-395	Unsupported	44	20	0.45	4087	47.62	0.76	46.97	0.11	155.1	0.10	<DL	0.04	0.92	<DL	0.02	<DL	0.13
ZQ15-072	Unsupported	19	16	0.85	5009	745.85	6.56	8.73	<DL	1.60	0.09	<DL	0.24	0.36	0.04	<DL	0.25	0.23
ZQ15-110	Unsupported	22	16	0.75	4837	1278.26	12.03	22.99	0.07	1.52	0.54	28.32	0.30	0.39	0.02	<DL	0.28	1.28
ZQ15-128	Unsupported	26	17	0.64	4600	527.85	6.12	9.15	0.03	0.99	0.08	<DL	0.33	0.30	0.04	0.02	0.10	0.13
ZQ15-151	Unsupported	26	17	0.64	4597	122.82	1.39	7.92	0.13	1.67	0.23	79.43	0.43	0.43	1.66	0.07	<DL	0.45
ZQ15-186	Unsupported	21	16	0.77	4866	261.59	2.41	24.45	0.53	1.68	2.39	1.31	0.24	1.93	0.18	0.03	1.32	0.40
ZQ15-209	Unsupported	20	16	0.82	4949	371.76	3.27	7.62	0.08	2.02	0.41	4.18	0.22	0.34	0.02	<DL	<DL	0.11

Note: <DL: lower than detection limit.

italics: mineralized sample